Investigation of the Role of Tensile Forces in Cellular Response to Chemotherapeutic Agents

By

Sarah Schmitt

Submitted to the graduate degree program in Bioengineering and the Graduate Faculty of the University of Kansas in partial fulfillment of the requirements for the degree of Master of Science.

_____

Chair: Arghya Paul, PhD

_____

Sara Wilson, PhD

_____

Andrew Godwin, PhD

Date Defended: 16 November 2016

The thesis committee for Sarah Schmitt certifies that this is the approved version of the following thesis:

Investigation of the Role of Tensile Forces in Cellular Response to Chemotherapeutic Agents

Chair: Arghya Paul, PhD

Date Approved: 16 November 2016

Abstract

Research using *in vitro* cell cultures are frequently conducted under static growth conditions. Cells growing *in vivo*, however, grow in a highly dynamic and interactive environment, where they receive cues in the form of mechanical stimuli from their surroundings. Lung cells, for example, are continually exposed *in vivo* to a cyclic tensile stretch during normal inhalation and exhalation. The absence of a mechanically representative environment could have important implications for research and development, particularly in the context of drug discovery. We hypothesize that tensile (mechanical) forces applied to two non-small cell lung cancer cell lines, bronchoalveolar H358 cells and alveolar A549 cells, play an important role in determining cellular response to chemotherapeutic agents. In order to investigate changes resulting from exposure to tensile stretch, we first looked at changes in proliferation and expression of a few cellular markers associated with epithelial-mesenchymal transition (EMT). Next, we looked at changes in cell cycle distribution and expression of a few cell-cycle checkpoint proteins. Finally, we studied the effect of a tensile force on the efficacy of three chemotherapeutic agents. We found that a tensile force significantly reduces cellular proliferation and causes significant shifts in cell cycle distribution. Mechanically active culture environments led to decreased efficacy of cisplatin and increased efficacy of Zactima. These results indicate that a mechanically active culture environment does impact cell survival and protein expression, and has important implications in the context of the discovery and screening of new antitumor drug therapies.

Acknowledgements

First, I would like to express my sincere gratitude to Dr. Arghya Paul for his continued support and motivation. His knowledge and guidance helped me throughout completion of this thesis, and I could not be more grateful. I would also like to thank Dr. Andrew Godwin and Dr. Sara Wilson for their insightful comments and continued encouragement throughout this process. I thank Dr. Gurusingham Sitta Sittampalam and Dr. Victor Sanjit Nirmalanandhan for providing me with the opportunity to join their team and conduct this research under their expertise, and expanding my interest in and knowledge of this fascinating field. I thank my fellow lab mates, past and present, for the interesting discussions, working together all of those long nights in the laboratory, and fun we have had the past few years. Last, but certainly not least, I would like to thank my friends and family for providing their unwavering support through many long evenings in the lab, many late nights writing, and life in general; you have meant so much to me, I cannot thank you enough. To each and every one of you, I could not have done this without you.

Table of Contents

List of Figures

List of Tables

Chapter 1: Introduction

1.1 Background and Rationale

Lung cancer is expected to account for approximately 14 % of new cancer cases and over one quarter of cancer deaths in 2016, making it the leading cause of cancer death in both men and women [1]. Of those lung cancer cases, approximately 85 % will be non-small cell lung cancer (NSCLC), indicating a continued strong need for therapies that are capable of effectively targeting the diverse types of NSCLC [2]. During the discovery for a new drug candidate, *in vitro* and *in vivo* experiments are conducted to establish the drug candidate's activity, efficacy and safety before proceeding to clinical trials. Animal models have long been beneficial and integral components of pre-clinical drug studies for the development of new drugs of all types, however, 85 % of novel drugs do not survive the transition from pre-clinical *in vivo* animal model to human clinical trials [3]. Aside from ethical concerns involved, the use of animal models is very costly financially but carries poor predictive power for which drugs will successfully make the translation from pre-clinical animal model to human clinical trial, due at least in part to substantial differences in cellular pathways and gene expression patterns that exist between species. There is a need for testing approaches that are able to more reliably predict efficacy and safety of new drug candidates in humans [4, 5], and the development of *in vitro* systems that serve as better organ-level mimics of *in vivo* human cellular conditions could potentially be an attractive supplement, if not eventual alternative, to existing drug discovery models.

Traditional *in vitro* studies have involved culturing cellular monocultures in plastic tissue culture plates. While this approach has served a beneficial purpose, it fails to capture the complex environment cells experience in the body, where cells exist in a dynamic three-dimensional world interacting with other cell types, non-cellular materials, and a variety of mechanical stimuli. New developments are pushing pre-clinical experimental model development toward cellular co-

cultures, more complex tissue cultures, and more complex three-dimensional environments [6], however, the development of representative models that capture the complexity of an *in vivo* environment in an *in vitro* context is still in its infancy. The integration of mechanical stimulation with cell culture is an important step in further bridging the gap between the dynamic *in vivo* environment and traditionally static *in vitro* culture models.

1.2 Mechanotransduction

The body is a dynamic cellular environment, with cells continuously being exposed to a variety of mechanical signals. The respiratory system, specifically the lung, is one marked example of the dynamic nature of the body, with lung cells continually experiencing various types of mechanical forces with each inhalation and exhalation. The airway, including the bronchus, bronchioles and the alveoli, experience shear forces as air flows into the lungs, and epithelial cells experience both tensile and compressive forces during each inhalation and exhalation. Very briefly, the epithelial cells that comprise the airway attach to the extra-cellular matrix, a complex network of locally-secreted proteoglycans, collagens and matrix proteins, such as laminin and fibronectin, through cell adhesion receptors on the cellular surface that span the cellular plasma membrane. These cell adhesion receptors connect via intermediary proteins to the interior of the cell to various microfilaments of the cytoskeleton, such as actin filaments and intermediate filaments. This coupling of the extracellular matrix to intracellular cytoskeletal elements allows for the transmission of external physical cues to the interior of the cell, ultimately affecting cellular changes at the nuclear level that effect all aspects of a cell's life, from gene expression to cellular positioning and motility, to cell division [7]. A generalized schematic of cellular mechanotransduction is depicted in Figure 1.

Much of our understanding of mechanotransduction began with animal studies, and many *in vivo* animal studies of the lung have focused on studies of fetal development. Fetal breathing movements are important for the normal development of lung, and our current understanding of

the importance of fetal breathing movements is heavily dependent on previous work done in animal models. A variety of *in vivo* approaches have been taken toward understanding lung development, and each of these has led to a deeper understanding of the importance of mechanical forces in the developing lung.

The lungs are filled with fluid during development, and small changes in the fluid volume and pressure allow for a controlled lung expansion and contraction that is important for formation of a healthy lung. Early studies of fetal sheep showed the importance of *in utero* lung fluid flow that accompanies fetal breathing movements through controlled expansion and contraction of developing lung tissue on healthy lung growth [8-11], and the cessation of breathing movements through a variety of means results in hampered lung development [12-16]. These studies helped to show us that a mechanically active environment was necessary for normal lung development and laid the groundwork for a basic understanding of lung mechanotransduction, but were limited in their ability to elucidate cellular activity associated with mechanical stimulation. Deconvolution of the mechanisms behind the treatment and the observed effect can be challenging on larger whole-organism level studies. Understanding mechanotransduction at cellular-level necessitate the precision and more tightly controlled conditions of *in vitro* models, and these factors contribute to the decreased popularity of animal models in mechanotransduction studies. Although no *in vitro* models perfectly mimic *in vivo* mechanical forces, bioreactors can be used to simulate breathing and study their cellular effects *in vitro*.

1.3 Bioreactors as In Vitro Models

Bioreactors are often used to simulate various types of *in vivo* forces such as tensile, compressive, and shear forces and perform *in vitro* studies to understand the effects of applied forces on cellular behavior. In order to mimic the motion of the lung during respiration, lung cells are often subjected to cyclic tensile forces. With this approach cells are typically cultured on a flexible elastomeric membrane, such as polydimethylsiloxane (PDMS), covalently coated with a

basement membrane component. A cyclic tensile force is then applied in one or more directions, allowing for physical manipulation of the cellular substratum in order to simulate the desired mechanical effect, which cells experience through interaction with the substratum as well as with neighboring cells.

Selection of the appropriate mechanical force profile is important when attempting to mimic the dynamic nature of the *in vivo* conditions in an *in vitro* model. Although the precise change in surface area experienced by cells in the lung *in vivo* remains unclear, cellular injury *in vitro* has been shown to occur when changes in cell surface area exceed 37 % [17, 18], a magnitude corresponding to inhalation greater than total lung capacity. The frequency of changes to cellular surface area in cyclic stretch profiles leads to cell damage primarily within the first few minutes of exposure to stretch, and cell damage increases with increased amplitude and magnitude [18]. Changes in cellular surface area up to 30 %, however, do not injure cultured cells [18, 19].

Applying a uniaxial stretch is one widely used approximation to study the effect of mechanical forces on lung cells. In this approach, cells are cultured on elastomeric strips or chambers and stretched from one or both ends, delivering a homogeneous tensile force to the cells along a single axis. Uniaxial stretch has been applied to cells grown on fibronectin-coated silicon chambers [19], strips of intact lung tissue [20], or in bending dishes that are physically stretched from above over loading supports [21]. The uniaxial stretching of cells and tissues has provided much insight into lung biomechanics and biochemical behavior, however, it does not necessarily provide a representative model of the forces experienced by lung tissue *in vivo*.

The use of biaxial distension adds force in an additional direction in an attempt to better model *in vivo* mechanical forces *in vitro*. Vacuum pressure has been applied directly to plastic petri dishes to deliver a tensile or compressive force along two axes [22]. More modernly, a flexible membrane acts as a cellular substratum through which mechanical stimulation is delivered. Polydimethylsiloxane (PDMS) membranes are frequently used in such a context, and have been

used as a mounting surface for precision-cut tissue slices [23] or as a cell culture surface built into multi-well culture plates. The plates are used in conjunction with a bioreactor designed to distend the flexible bottoms of the plates, delivering both circumferential and radial strains to the cultured cells. The application of a biaxial force to cells has been accomplished through a convex deflection of the culture surface from below using air [24] or liquid [25, 26], through pushing the culture surface down over a post [27], or driving a piston upward to stretch the culture membranes [28]. One common methods employed involves the use of vacuum pressure to pull the culture membranes down over a fixed post. The Flexcell strain unit (Flexcell International), one commercially available instrument commonly used in mechanotransduction studies, uses this approach. With the Flexcell device, cells are cultured in plastic six-well plates that contain flexible membranes as the bottom culture surface. Vacuum pressure is utilized to pull the flexible membranes down over a Delrin post using a force profile and frequency customizable through a software interface. Flexcell units have been used rather extensively to study the effects of mechanical strain on lung cell differentiation [29-31], proliferation [32, 33], [34], and gene expression [35-37], to list a few examples. The ability to provide a biaxial stretch to cultured cells is an improvement over application only along a single axis, and its use for lung epithelial cell culture is the focus of this thesis.

1.4 Description of Cell Culture

For each of the studies described in this thesis, the FX-4000 Flexcell Tension Plus system by Flexcell International Corporation was used to apply a tensile strain to cultured cells. All cells were cultured in 35 mm diameter, 6-well BioFlex plates with flexible silicone elastomer well bottoms. Well bottoms were pre-coated with covalently bonded Collagen I to promote cellular adhesion. Cells were allowed to grow for 24 hours prior to the administration of tension to promote cellular adhesion to the well surface.

After 24 hours, plates in the mechanically active culture groups were loaded on Equibiaxial loading stations, designed to apply a uniform radial and circumferential strain to cells. Each six-well culture plate fits in a gasket in one of four positions available on the loading station base. Each well of the plate fits over a Delrin planar-faced cylindrical loading post 25 mm in diameter; when vacuum is applied to the loading station base the well bottoms deform across the loading post face, creating equibiaxial strain (see Figure 2 for the base station assembly). A thin layer of Loctite silicone lubricant is applied to the top and sides of each loading post prior to assembling culture plates in the loading station. A plexiglass cover is applied to the top of assembled loading stations, and a 5 to 10-pound weight is applied to the top of the plexiglass cover to ensure culture plates remain firmly seated in the base station. The entire base station assembly is housed in a cell culture incubator at 37 °C, a 5 % CO_2 concentration and 95 % relative humidity.

Vacuum pressure is applied using a Leybold Trivac B vacuum pump controlled by a software interface. Cells exposed to forces were subjected to a half-sinusoidal cyclic strain profile of 20% maximum membrane elongation at 0.5 Hz frequency per step (2 second elongation followed by 2 seconds relaxation, or 15 cycles per minute with an average strain of 10% per cycle). Cells cultured under static conditions in these experiments were cultured in the flexible-bottom six-well culture plates described for the mechanically active culture groups, but were not connected to vacuum pressure. See Figure 2 for a basic overview of the cell culture and tension delivery mechanism used for these studies.

1.5 Project Scope

This thesis examines the effect of simulated *in vivo* mechanical stimulation on *in vitro* cultured cells with an eye toward its utilization in a drug-discovery context. Two non-small cell lung cancer cell lines in particular were investigated: H358, a bronchoalveolar cell line, and A549, a pulmonary epithelial cell line. Chapters 2 and 3 report findings related to a few general biological changes that occur with mechanically stimulated cells *in vitro* with respect to proliferation. Chapter 2 looks

at proliferative and morphological changes occurring with exposure to mechanical stimulation, then at changes in cellular levels of a few proteins associated with cellular epithelial-to-mesenchymal transition. Chapter 3 targets cell cycle changes that occur with stimulation; changes in the number of cells present in each stage of the cell cycle are examined and proteomic changes in a few key cell cycle proteins are investigated. Chapter 4 discusses *in vitro* drug studies conducted in a mechanically active culture environment with a few different chemotherapeutic agents, with particular attention to proliferative changes observed. Chapter 5 then provides general conclusions and recommendations based on these findings.

Chapter 2: Proliferative and Morphological Changes Accompanying *In Vitro* Mechanical Stimulation

2.1 Introduction

Much *in vitro* research has been conducted using bioreactors to study the relationship between lung dynamics and cellular behavior, and many of these studies have focused on the fetal development of lungs. Fetal breathing movements expose the lungs to mechanical forces even before they serve the purpose in gas exchange, and play an important role in fetal lung development [38].

Fibroblasts play an important role in extracellular matrix deposition and regulation of alveolar structure, and the role of mechanical stimulation in their proliferation is a subject of debate. Human lung IMR-90 fibroblasts showed an increase in proliferation when exposed to a cyclic biaxial stretch in two-dimensional cultures, and cellular replication is further increased in IMR-90 cells cultured in media extracted from the wells of mechanically stimulated cells [39]. In contrast, fibroblasts isolated from rats during the canalicular stage of development demonstrated a decrease in proliferation in response to a tensile force [40]. Liu et al. studied both two-dimensional cultures and “organotypic” cultures, three-dimensional co-cultures composed of mixed fibroblast and epithelial cells isolated from rats during the canalicular stage of lung development (at 19 days of gestation). While measurement of DNA incorporation of [3H] thymidine showed no significant change in proliferation in two-dimensional cultures, increases in proliferation in three-dimensional organotypic cultures in response to a cyclic uniaxial stretch were observed [41, 42]. The decreases in proliferation in two-dimensional fibroblast cultures [40] and the increases in three-dimensional organotypic cultures [41, 43] could be attributed to differences in the applied stretch (uniaxial or biaxial) or differences in cell-cell contacts between two and three-dimensional cultures [43]. Xu et al. reported that strain-enhanced proliferation is gestation dependent, with proliferation being the highest during the early canalicular stage at 19 days of gestation; this gestational response to mechanical force appears to be regulated by cellular interactions with the

mesenchyme [44]. These mostly undifferentiated and loose connective tissue cells of mesodermal origin easily migrate and may have different responses to drugs when compared to cells of epithelial origin. Epithelial-mesenchymal transitions and vice versa (mesenchymal-epithelial transitions) are critical in cancer pathology; hence the effect of forces could be important in research and development applications in oncology.

2.2 Methods

2.2.1 Cell Culture

The bronchoalveolar line NCI-H358 (ATCC) and the alveolar adenocarcinoma line A549 (ATCC) were obtained from American Type Culture Collection (ATCC). H358 cells were cultured in RPMI-1640 (Sigma Aldrich) and A549 cells were cultured in HAM's F12K (ATCC). Both were supplemented with 10% Fetal Bovine Serum (Sigma Aldrich) and 1% Penicillin Streptomycin (Sigma Aldrich). Cells were passaged in 75 cm2 culture flasks at 37° C in 5% CO_2, and trypsinized using TrypLE Express containing phenol red (Gibco). Both cell lines were individually cultured in six-well Bioflex Collagen I plates (Flexcell International). H358 cells were seeded at 100,000 cells/well and A549 at 20,000 cells/well for both static wells and wells exposed to forces as described in Chapter 1.4.

2.2.2 Application of Mechanical Stimulation

Cells were allowed to attach to the plate for 24 hours prior to the application of forces. After 24 hours, a FX-4000 Tension plus unit (Flexcell International) was used to apply a tensile force to cells. Cells exposed to forces were subjected to a cyclic strain of 20 % maximum strain for 2 seconds, followed by 2 seconds of rest (15 cycles per minute with an average strain of 10 % per cycle). The total duration of the experiment was 144 hours.

2.2.3 Cell Harvesting and Counting

Cells were harvested from each well individually at two time points, 72 hours and 144 hours, using TrypLE (Gibco) and transferred to new labeled six-well plates in order to maintain treatment group identities. Briefly, media was removed from the culture wells to their corresponding new labeled six-well plates and 300 µL of TrypLE was added to each culture well. Each well's reserved media was then used to transfer dislodged cells from the culture wells to the new plates. The volume of each well was measured and brought up to a total volume of 4 mL using phosphate-buffered saline. Cell counts were then taken using 1 mL of cells/media from each well using a Vi-CELL Cell Counter (Beckman Coulter). The viable cell count was then converted to a cell count per original 4 mL well by multiplying each cell count by four. Results shown are mean viable cell counts plus or minus the standard deviation. Differences in viable cells counts between static cell cultures and dynamic cultures at each time point were statistically analyzed with GraphPad Prism Version 5.04 (GraphPad Software, Inc.) using a two-tailed Student's t-test with Welch's correction. Significance was set at $p < 0.05$. The experiment was repeated on three separate days.

2.2.4 Morphological Examination

Sample wells for both cell lines were visually examined at two time points: at 72 hours and at 144 hours. Visual examination was conducted using an Olympus IX71 inverted microscope with 10x objective lens, and representative pictures taken for each cell line and each forces group at both time points.

2.2.5 Western Blotting of Select EMT Markers

Whole cell lysates were created for both cell lines at both 72 hours and 144 hours, and western blotting was conducted for selected protein markers associated with either an epithelial phenotype or a mesenchymal phenotype. Cells were harvested using TrypLE Express followed by centrifugation at 200 x g at 4 °C. Cell pellets were resuspended and washed three times with cold PBS (Gibco). Cells were then resuspended in RIPA buffer (Sigma Aldrich) and lysed using

three freeze/thaw cycles alternating between liquid nitrogen and a 37 °C water bath. Protein concentrations were determined using a Detergent Compatible (DC) Protein Assay (Bio-Rad). A total of 30 µg of each protein sample was mixed with E-PAGE loading reagent (Invitrogen) and NuPAGE reducing reagent (Invitrogen). Samples were heated at 95 °C for 5 minutes and loaded in wells of 8% E-PAGE gels (Invitrogen). The separated proteins were then transferred to nitrocellulose using iBlot transfer stacks (Invitrogen). Blots were blocked in 0.1 % Tween in Tris-buffered saline with either 5% bovine serum albumin or 5 % milk for 1 hour at room temperature. Blots were then incubated with antibodies to E-cadherin, β-catenin, γ-catenin, Vimentin, N-cadherin, or Fibronectin at 1:500-1:1000 (all Santa Cruz Biotechnology, Inc.) at 4 °C overnight. Beta-actin was used as a loading control at 1:3000 (Abcam). All blots were washed and incubated with a corresponding secondary IgG-HRP linked antibody, either goat anti-rabbit (Santa Cruz Biotechnology, Inc.) or goat anti-mouse (Santa Cruz Biotechnology, Inc.) for two hours at room temperature, then incubated with Immobiolon Western Chemiluminescent HRP substrate (Millipore) according to manufacturer's instructions. Images were obtained using an AutoChemi System (UVP BioImaging Systems).

2.3 Results

2.3.1 H358 Bronchoalveolar Epithelial Cells Fail to Proliferate with Mechanical Stimulation

At 24 hours, just prior to the application of forces to the "With Forces" group, viable cell counts for the statically cultured cells and cells cultured with tensile stretch show no significant differences. Shortly after the application of forces to the "With Forces" group, however, the viable cell count numbers stagnate. The "Without Forces" group viable cell count numbers show a roughly exponential growth pattern, whereas the group exposed to tensile stretch did not. Significant differences in viable cell counts between statically cultured cells and cells grown under stretched conditions appeared at 48 hours, and continued at throughout the duration of the experiment through the 144-hour time point (Figure 3).

2.3.2 H358 Bronchoalveolar Epithelial Cells Detach and Form Aggregates with Mechanical Stimulation

Morphological examination of representative wells for both the “With Forces” and “Without Forces” group at 72 hours. The “With Forces” group showed detachment of H358 cells from the plate membrane surface and formation of cellular clusters, or spheroidal type aggregations. These cellular aggregations were still present at the 144-hour time point (Figure 4).

2.3.3 A549 Alveolar Epithelial Cells Fail to Proliferate with Mechanical Stimulation

At 24 hours, similar to proliferation results for H358 cells above, viable cell counts differ only slightly between cells cultured in static plates and cells cultured with a cyclic tensile force. However, again similar to the H358 cell proliferation results, viable cell count numbers fail to increase in the “With Forces” group. The “Without Forces” group again shows viable cell count numbers that increase roughly exponentially, leading to significant changes in cell counts between cells cultured with tensile stretch and without tensile stretch at 72 hours and continuing through 144 hours (Figure 5).

2.3.4 A549 Alveolar Epithelial Cells Remain Adherent with Mechanical Stimulation

Morphological examination of representative wells for both the “With Forces” and “Without Forces” group at 72 hours. Both the “With Forces” and “Without Forces” groups remained adherent through both time points (Figure 6).

2.3.5 Increased Epithelial Marker E-cadherin and Decreased Mesenchymal Markers with Mechanical Stimulation of Bronchoalveolar Epithelial Cells

For H358 cells exposed to stretch, a modest increase in the epithelial marker E-cadherin was observed at both 72 hours and 144 hours (Figure 7a). Mesenchymal markers vimentin and fibronectin showed decreased levels with exposure to stretch, with vimentin levels decreased at 72 hours with forces, and fibronectin levels decreased at 144 hours with forces (Figure 8a).

2.3.6 Decreased Epithelial Marker β-catenin and Increased Mesenchymal Markers Vimentin and N-cadherin with Mechanical Stimulation of Alveolar Epithelial Cells

For A549 cells, β-catenin was decreased in stretched cells at 144 hours, though expression was low for both stretched and unstretched cells at 144 hours compared to that at 72 hours (Figure 7b). Vimentin appeared increased in stretched cells at 144 hours and N-cadherin increased in stretched cells at both time points (Figure 8b).

2.4 Discussion

An approximately exponential growth profile was observed in both cell lines without the presence of a cyclic stretch. Each cell line has a very different growth rate; seeding densities were adjusted to yield approximately equivalent cell counts in both lines in non-stretched cells at the end of the experiment. In the presence of cyclic stretch, both cell lines showed a “stagnation” of proliferation. Cells exposed to stretch failed to proliferate. The morphological changes observed with these two cell lines were interesting, as they were different for each line. The H358 cell line formed three-dimensional aggregates that were detached from the surface of the plate. This behavior was observed at both time points in the experiment. It is possible that the cells exposed to stretch were dying and detaching from the plate, but dead and detached cells would not necessarily be expected to form and maintain spheroidal aggregates. Cells, alternately, may have been detaching from the plate while still alive. The exposure to stretch could have altering expression of cell surface proteins that play a role in cell-cell interactions and cellular adhesion to the plate membranes. This was not observed in the A549 cell line, which stayed adherent to the plate at all time points and under all mechanical culture conditions. The changes in protein expression may lend some clues to the changes in morphology observed in H358 cells with stretched culture conditions. Cells secrete fibronectin into the extracellular matrix where it binds ECM components such as collagen. Decreased levels of fibronectin at 144 hours in the H358 cell line would mean less binding to collagen, which could help explain the detachment observed.

H358 cells also showed increased E-cadherin levels, a molecule heavily involved in cell-cell interactions, at both time points. This again fits with the observed aggregation of these cells, which would involve increased cell-cell contact. Whether the detachment preceded the changes in fibronectin and E-cadherin expression or vice versa, however, remains unknown.

Little change in protein expression of E-cadherin, β-catenin, or γ-catenin was observed between active and static cultures in A549 cells, though mechanically active cultures of A549 did show increases in N-cadherin levels at both time points, and increases in vimentin levels at 144 hours. Increased N-cadherin and increased vimentin levels are associated with epithelial-mesenchymal transition (EMT), a critical process by which malignant tumors become more invasive and develop metastases. Decreases in epithelial markers such as E-cadherin, β-catenin, and γ-catenin and increased levels of mesenchymal markers including vimentin, N-cadherin, and fibronectin are all signs in a cellular shift from an epithelial to mesenchymal phenotype. Increased E-cadherin at all time points coupled with decreased Vimentin levels at 72 hours and decreased fibronectin at 144 hours in the already more-epithelial like H358 cell line in mechanically active cell culture hint toward this cell line acting even more epithelial-like, and so showing less signs of EMT, with simulated *in vivo* forces. Similarly, the more mesenchymal A549 cell line displayed EMT marker levels consistent with a more mesenchymal phenotype in mechanically stimulated cells through increased vimentin at 72 hours and increased N-cadherin at all time points.

One potentially important limitation of this study concerns the dissociation of cells from the plate culture membranes. Since some fraction of H358 cells are detaching from the plate, the detached cells are not experiencing the desired tensile strain. The strain applied to cells in this experiment was, at 20 %, relatively high. This high level of strain may itself potentially impact cellular adhesion to the plate membranes as well as cellular response to an applied strain. Decreasing the strain applied to cells may help to mitigate the observed detachment of H358 cells from their culture surfaces. A study of the application of varying stretch profiles could be used

toward this end. The application of varying stretch profiles could additionally provide information regarding changes in cellular response with changing amounts of stretch. The detached clusters of cells floating in the media may likely instead be experiencing some fluid flow stimulation due to any movement of the media that accompanies the cyclic distension of each well. The effects of this type of stimulation were not within the scope of this project, but could be interesting to investigate in its own right. Questions as to how stimulation of cells leads to detachment, whether through physical damage to cell-matrix interactions, through changes in expression of ECM-interacting proteins as observed above, activation of the secretion of matrix metalloproteinases or other extracellular matrix degrading enzymes [45], or through some other means still remain to be answered.

Relating to the previously mentioned limitation of cellular detachment, the method used to determine cell viability for this study is itself another potential limitation. Trypan blue exclusion was utilized to determine viable cell counts, but as this method stains intact cells, it cannot be used to distinguish between cells that are healthy and cells that are alive but losing the ability to function normally. An assay utilizing cellular metabolic capability for determining cellular viability, such as CellTiter-Blue, for example, would be able to distinguish between healthy cells and intact cells with diminishing functionality, making this a good inclusion for the proliferation study conducted here.

In conclusion, a marked change in proliferation was observed with exposure to a cyclic tensile stretch, and this was coupled with shifts in EMT marker expression in both cell lines. Though the shifts in EMT marker expression may help explain some of the cellular detachment observed in stretched cells, these shifts do not readily speak to the proliferative stalling we observed in both cell lines. This led us to question how cell cycle progression is impacted by exposure of cultured cells to a mechanical stretch; a study of cell cycle progression is the focus of Chapter 3.

Chapter 3: Changes in Cell-Cycle Progression in Mechanically Active Cell Cultures

3.1 Introduction

Normal cellular proliferation involves the proper coordination and control of events during cell cycle progress, with the loss of cell cycle control leading to conditions such as cancer. Mechanical forces have been shown to affect the proliferation of cells by altering the progression of events at differing stages in the cell cycle [40, 46-49]. Increases in proliferation have been seen human lung fibroblasts [50], airway smoot muscle cells [32, 51], and lung epithelial cells [33, 34, 39, 41] with exposure to a cyclic stretch. In cultured vascular smooth muscle cells, a cyclic strain causes a G1/S cell cycle arrest [46]. Sedding et al., however, used cyclic strain to instead promote entry of quiescent vascular smooth muscle cells into the cell cycle [47]. A G2/M accumulation has been observed in cardiac fibroblasts exposed to cyclic strain [48], and fetal rat lung fibroblasts show decreased proliferation and increased apoptosis [40]. Fetal rat lung epithelial cells exhibit increased CDK inhibitor protein expression and nuclear localization in response to stretch, resulting in a G1 cell cycle arrest *in vivo* [49]. A variety of responses to mechanical stimulation have been observed; the results are far from clear-cut. Despite advances in knowledge regarding how mechanical stimulation affects cell cycle progression in a variety of cell types, the effect of mechanical stimulation on cell cycle progression in cancer cells, cells notable for possessing altered cell cycle controls, remains largely unexamined.

The role of changes in cell cycle controls and apoptosis have been investigated as mechanisms behind the observed changes in proliferation in response to mechanical forces [40, 46, 52]. Cells progress through well-defined stages during the cell cycle prior to mitosis. The orderly duplication of non-chromosomal cellular contents in the G1 phase, followed by the duplication of chromosomes in the S phase, is necessary for mitosis and the proliferation of cells. Inhibition of a G1/S phase transition has been observed in vascular smooth muscle cells in

response to cyclic stretch [46]. In a similar study, Sanchez-Esteban et al. observed significant increases in quiescent (G0) and G1 phase cells and significant decreases in S phase cells in biaxially stretched fibroblasts, indicating an inhibition of cell cycle progression [40]. The enhanced apoptosis observed is due to increased caspase-3 activation under stretched conditions [40, 52]. This evidence suggests that stretch may serve as a mechanism for controlling proliferation and guiding normal lung development by inducing increases in apoptosis and changes in cell cycle signaling events.

The uncontrolled proliferation that occurs in cancer results for a loss of ability to regulate cell cycle progression [53, 54]. In fact, cancer can be viewed as a disease of the cell cycle. A large number of therapies designed to target cancer that are currently in use are mitotic inhibitor that target actively proliferating cells. The effectiveness of anti-cancer therapies that target actively proliferating cells, then, may be altered by changes in cell cycle progression that result from exposure to a repeated mechanical stimulus. During the drug discovery process, many potential anti-cancer agents are promising against cells grown under static conditions, but fail as they are moved to animal models that serve as a more physiologically representative environment. Ailments such as lung cancer involve the aberrant growth of cells in a mechanically active environment, and so studies conducted on statically grown cells may not be capturing the whole clinically relevant picture. An understanding of mechanotransductive pathways and cellular responses to strain, particularly in the lung, may prove to be beneficial in the area of drug discovery. To this end, this cell cycle experiment was conducted to examine changes in cell cycle accumulation due to culture in a mechanically active environment. The distribution of cells in each phase of the cell cycle, G0/G1, S, G2, or M phase, was determined using flow cytometry. To further understand the changes in cell cycle distribution observed, western blotting was used to determine changes in the relative expression of three cell cycle related proteins important for M-

phase progression: Cyclin B1, CDK1, and p21 (see Figure 9 for a generalized depiction of the cell cycle and checkpoint proteins in this study).

3.2 Methods

3.2.1 Cell Culture

Two non-small cell lung cancer (NSCLC) lines, a bronchoalveolar line NCI-H358 (ATCC), an alveolar adenocarcinoma line A549 (ATCC), and a non-tumorigenic lung cell line, NL-20 (ATCC), were obtained from American Type Culture Collection (ATCC). H358 cells were cultured in RPMI-1640 (Sigma Aldrich) and A549 cells were cultured in HAM's F12K (ATCC). Both were supplemented with 10% Fetal Bovine Serum (Sigma Aldrich) and 1 % Penicillin Streptomycin (Sigma Aldrich). NL-20 cells were cultured in HAM's F12K media supplemented with 2.7 g/L glucose (Sigma Aldrich), 0.1 mM nonessential amino acids (Sigma Aldrich), 0.005 mg/ml insulin (Sigma Aldrich), 10 ng/ml epidermal growth factor (Sigma Aldrich), 0.001 mg/ml transferrin (Sigma Aldrich), 500 ng/ml hydrocortisone (Sigma Aldrich), and 4% Fetal Bovine Serum (Sigma Aldrich). Cells were passaged in 75 cm^2 culture flasks at 37 °C in 5 % CO_2, and trypsinized using TrypLE Express containing phenol red (Gibco).

All three cell lines were individually cultured in six-well Bioflex Collagen I plates (Flexcell International). A differential seeding density was again used for each cell line to achieve an approximately equivalent degree of confluence after three days as described in Chapter 1.4. NL-20 cells showed growth rates comparable to H358 cells, so the seeding density used for H358 was adopted for NL-20 in this study. Both H358 and NL-20 cells were seeded at 100,000 cells/well for static cells and 170,000 cells/well for the group exposed to forces. A549 cells were seeded at 20,000 cells/well for static cells and 35,000 cells/well for cells exposed to forces.

3.2.2 Application of Mechanical Stimulation

Cells were allowed to attach to the plate for 24 hours prior to the application of forces. After 24 hours, a FX-4000 Tension plus unit (Flexcell International) was used to apply a tensile force

to cells, as described in Chapter 1.4. The duration of exposure to forces was either 48 hours for the 72-hour group, or 120 hours for the 144-hour group.

3.2.3 Cell Cycle Analysis

In order to examine the effect of an applied mechanical strain on cellular proliferation, we looked at the effect on cell cycle progression. Flow cytometry was used to determine the number of cells in G0/G1, S, G2, and M phases. Asynchronous cells were harvested from plates using TrypLE (Gibco). Cells were pelleted at 1000 rpm and washed with phosphate buffered saline (PBS) three times, then fixed in cold 90% ethanol in PBS overnight. Fixed cells were then centrifuged and resuspended in staining buffer supplemented with fetal bovine serum (BD Biosciences). To determine the number of cells in M-phase, cells were stained with rat anti-histone H3 pS28 conjugated to BD Horizon V450 (BD Biosciences), then treated with a solution of propidium iodide containing RNase (BD Biosciences), as described previously [55]. The percentages of cells in each phase of the cell cycle were then determined with a BD LSR II flow cytometer (BD Biosciences) using BD FACSDiva software (BD Biosciences). Each analysis was conducted on separate days a minimum of three times. Flow cytometry data graphs were created and statistical analysis conducted with GraphPad Prism Version 5.04 (GraphPad Software, Inc.) using a Student's two-tailed unpaired t-test with significance set at $p < 0.05$. Each experiment was repeated a minimum of three times.

3.2.4 Western Blotting

In order to follow up on cell cycle progression changes observed in the cell cycle analysis conducted using flow cytometry, particularly the changes in percentages of cells in M-phase, western blot analyses on whole cell lysates were conducted for p21, CDK1, and cyclin B1 expression. Because significant changes in cell cycle progression were not observed in the non-tumorigenic NL-20 cell line, only NCI-H358 and A549 cells were examined using western blotting. Cells were harvested using TrypLE Express followed by centrifugation at 200 x g at 4 °C. Cell

pellets were re-suspended and washed three times with cold PBS (Gibco). Cells were then re-suspended in RIPA buffer (Sigma Aldrich) and lysed using three freeze/thaw cycles alternating between liquid nitrogen and a 37 °C water bath. Protein concentrations were determined using a Detergent Compatible (DC) Protein Assay (Bio-Rad Laboratories). A total of 30 µg of each protein sample was mixed with E-PAGE loading reagent (Invitrogen) and NuPAGE reducing reagent (Invitrogen). Samples were heated at 95 °C for 5 minutes and loaded in wells of 8% E-PAGE gels (Invitrogen). The separated proteins were then transferred to nitrocellulose using iBlot transfer stacks (Invitrogen). Blots were blocked in 0.1 % Tween in tris-buffered saline with either 5% bovine serum albumin or 5 % milk for 1 hour at room temperature. Blots were then incubated with antibodies to non-phosphorylated p21 at 1:200 (Santa Cruz Biotechnology, Inc.) non-phosphorylated CDK1 at 1:100 (Millipore) or non-phosphorylated Cyclin B1 at 1:200 (Santa Cruz Biotechnology, Inc.) at 4 °C overnight. Beta-actin was used as a loading control at 1:3000 (Abcam). All blots were washed and incubated with a corresponding secondary IgG-HRP linked antibody, either goat anti-rabbit (Santa Cruz Biotechnology, Inc.) or goat anti-mouse (Santa Cruz Biotechnology, Inc.) for two hours at room temperature, then incubated with Immobilon Western Chemiluminescent HRP substrate (Millipore) according to manufacturer's instructions. Images were obtained using an AutoChemi System (UVP BioImaging Systems).

3.3 Results

3.3.1 H358 Cells Showed Increased G0/G1 and Decreased G2 Phase H358 Cells After 72 Hours, But Decreased S-Phase and Increased M Phase at 144 Hours

At the 72-hour time point, H358 cells exposed to forces showed a greater percentage of cells in G0/G1 than cells cultured statically, but showed fewer cells in G2 phase as compared to statically cultured cells (Figure 10a). This corresponded with increases in non-phosphorylated CDK1, cyclin B1, and p21 with a tensile stretch (Figure 10b). After 144 hours, a significant decrease in the percentage of cells in S phase was seen in stretched cells relative to unstretched

cells. The percentage of cells in M-phase in stretched cells was significantly increased relative to unstretched cells (Figure 10c). At 144 hours, levels of CDK1 and cyclin B1 in H358 cells exposed to a cyclic tensile force were relatively constant in comparison to non-stretched cells, while levels of p21 were increased (Figure 10d). Flow cytometry results for all are summarized in Table 1.

3.3.2 A549 Cells Showed Increase Mitotic-Phase Cells after 72 Hours, but Decreased G0/G1 and S-Phase Cells after 144 Hours

In A549 cells, there was a significant increase in M phase cells in cells grown with a tensile stretch relative to unstretched cells after 72 hours of forces (Figure 11a), corresponding with increases in cyclin B1, CDK1 and p21 at the 72-hour mark in mechanically active cell cultures (Figure 11b). Cells cultured with stretch showed a significant decrease in the percentages of cells in G0/G1 relative to statically cultured cells. S-phase distribution of cells was also decreased in stretched cells versus unstretched cells after 144 hours (Figure 11c). At 144 hours, decreased relative amounts of p21, cyclin B1, and CDK1 were seen (Figure 11d). Flow cytometry results for all are summarized in Table 1.

3.3.3 NL-20 (Non-Tumorigenic) Cells Showed No Significant Changes In Cell Cycle Distribution

NL-20 cells exposed to a cyclic distension did not show significant changes in the percentage of cells in any phase at either the 72-hour (Figure 12a) or the 144-hour (Figure 12b) time points. Flow cytometry results for all are summarized in Table 1.

3.4 Discussion

The purpose of this study was to investigate the effect of an applied cyclic tensile force on the distribution of cells in M-phase in one non-tumorigenic lung epithelial cell line and two non-small cell lung cancer lines. Normal progression of the cell through the various phases of the cell cycle requires a carefully timed orchestration of events between numerous proteins that work to either promote or inhibit cell division at different points in the cell cycle. Cyclins and cyclin-

dependent kinases (CDKs) in particular work as partners to control cell cycle progression. Members of the cyclin B family and CDK1 (cdc2) in particular interact to promote the entry of cells into G2/M. Their activity remains important through mitosis for spindle assembly [56] and deactivation of the Cyclin B1-CDK1 complex is necessary for mitotic completion. The cyclin-dependent kinase inhibitor p21 works as a counterbalance to cyclin-CDK activity, inhibiting the activity of cyclin-CDK complexes throughout the cell cycle. The improper regulation of cell cycle protein levels and activity can result in loss of cell cycle control, leading to the uncontrolled proliferation that defines cancer cells.

Although no significant changes were seen in the non-tumorigenic lung epithelial line, both non-small cell lung cancer lines showed significant changes at differing time points. The link between the changes observed in protein expression and changes in cell cycle progression in these cancer lines are not immediately clear. A549 cells showed a significant accumulation of cells in M-phase at the 72-hour time point in stretched cells, but this M-phase difference between stretched and unstretched cells was eliminated at the 144-hour time point, indicating that the accumulation was temporary. The significant M-phase increase in H358 cells at the 144-hour time point was accompanied by an increase in p21. This could be consistent with the G2/M arrest seen previously in cardiac fibroblasts cultured under stretched conditions [48]. The results from Liao et al. supported p53 involvement in cardiac fibroblast G2/M arrest [48]. H358 cells, however, carry a homozygous p53 gene deletion [57, 58], indicating that another mechanism must control the increased expression of p21. One possible explanation is increased p21 leading to increases in cell cycle progression from G2 to M phase. Transient hyper-phosphorylated forms of p21 in the nucleus have been shown to increase cyclin B-CDK1 activity [59], which would drive cells through G2 into M-phase. However, our stretch-induced decline in proliferation indicates that cells are not merely entering M-phase with greater frequency, but are showing a proliferative decline. At the

very least, p21-induced activity of cyclin B1-CDK1 as describe above would not be the sole explanation to the cell-cycle changes observed here.

Another interesting possibility is induction of p21 independent of p53 through nuclear factor-κB (NF-κB) as suggested by Wuerzberger-Davis et al [60]. They found an increase in G2/M arrest through p21 induction in an NF-κB-related manner. Changes in NF-κB levels occur in response to integrin stimulation through MAPK activation, and increases in NF-κB have been observed in osteoblasts in response to cyclic tension [61]. Increased p21 mRNA expression mirroring the protein expression changes seen in H358 cells at both 72 hours and 144 hours have been observed by our group through RT-PCR analysis (data unpublished). This points to mechanical-stimulation exerting control of p21 protein expression at the transcription level, however, a direct link between H358 cell cycle changes and mechanically stimulated NF-κB transcription factor activation has not yet been investigated.

There are increased levels of cyclin B1, CDK1, and p21 in mechanically stretched A549 cells (relative to statically culture cells) stalled in M-phase after 72 hours. This trend is reversed at the 144-hour time point for all three proteins, with mechanically active A549 cultures showing decreases relative to statically cultured cells, though expression of cyclin B1, CDK1, and p21 are relatively consistent in mechanically active cell cultures at both time points. There are significant decreases in G0/G1 and S phase cells at 144 hours with forces, accompanied by small but not statistically significant increases in G2 and M phase cell counts. The return of M-phase cell counts to levels comparable to un-stretched cells at 144 hours without observed changes in relative levels cyclin B1, CDK1, or p21 indicate the M-phase changes are not directly linked to levels of these three protein regulators. Further studies will be necessary to track mechanisms behind the transient M-phase changes in A549 cells. The low cyclin B1 levels in both cell lines during M-phase accumulation could indicate some form of effective cyclin B1 depletion resulting in delays in mitotic completion. Cyclin B1 accumulates at kinetochores during prometaphase, where it plays

a role in spindle formation [56] forming the proper attachments between kinetochores and microtubules [62]. Low levels of cyclin B1, therefore, could retard spindle formation, stalling exit from the M-phase. In the case of A549 cells stalled at 72 hours, this again seems unlikely as the sole mediator of M-phase progression. A549 cells at 144 hours no longer showed significant changes in M-phase cell numbers between stretched and un-stretched cells, however cyclin B1 levels were decreased in stretched cells at 144 hours. This would indicate that cyclin B1 depletion alone is not responsible for M-phase changes in A549 cells. This could potentially fit with cyclin B1 levels and M-phase counts in H358 cells at 144 hours, though further investigation would be warranted.

That changes were seen in both cancer cell lines while none were observed in the non-tumorigenic epithelial line was intriguing. Successful cancer chemotherapeutic treatments often rely on shutting down cell division by attacking cancerous cells at specific phases in their cell cycles. Different cancers often have differing aberrations in their cell cycles that allow them to circumvent normal cell cycle controls in differing ways, contributing to the difficulty of developing new therapies.

To address a few limitations of this study, it is important to note that asynchronous cells were used throughout this cell cycle investigation. The use of asynchronous cells was due to the relatively long time period of the experiment, but the use of both synchronized cell cultures and a greater number of closer time points could be used to provide additional insight into changing cell cycle kinetics. Serum starvation prior to the addition of a mechanical stimulus could be used to create an accumulation of cells at G1, then subsequent reintroduction of serum into culture media would produce cells that are in cell cycle synchrony prior to the addition of a tensile stretch. A number of other methods of synchronizing cells could be used in this context to provide further information about changes in cell cycle distribution.

Another limitation of this study is the lack of identification of either quiescent or senescent cell populations. Detection of and discrimination between cells that are actively dividing, quiescent cells that are withdrawn from the cell cycle but are still cell cycle competent, and senescent cells that are permanently arrested can be accomplished through various staining methods for flow cytometry analysis. Such discrimination between cell populations could assist in contextualizing cell cycle accumulation shifts seen with mechanically active culture conditions, making quiescent and senescent cell detection potentially worthwhile inclusions in this and other similar studies.

In conclusion, we have found that mechanically active culture conditions cause changes in cell cycle phase accumulation in two lines of lung epithelial cells. The precise mechanisms behind the cell cycle changes still remain to be elucidated, but they appear to vary depending in part on the particular cell cycle abnormalities inherent in the cancer cell line in question. These results represent a starting point for further investigation into cell cycle perturbation as a result of mechanical stretch.

Chapter 4: Application of Chemotherapeutic Agents to a Mechanically-Active Culture Environment

4.1 Introduction

A very common approach to the treatment of cancer is chemotherapy. A chemical compound, or cocktail of multiple compounds, is delivered to the body with the intention of killing the aberrant cancerous cells. Particular chemotherapeutic approaches vary depending on the type of cancer present. One commonly used approach systemically targets all rapidly-dividing cells, cancerous or not, to induce cell death. Compounds used to induce the death of rapidly dividing cells accomplish this task using a few different approaches. Some agents work to prevent normal cytoskeletal behavior during mitosis, either through prevention of microtubule assembly in the case of vinca alkaloids, or prevention of disassembly in the case of taxanes. The functional assembly and disassembly of microtubules is required for successful partitioning of DNA into newly-forming cells during the mitotic phase of the cell cycle; when this fails apoptosis is triggered. Other approaches work through physical alteration of DNA structure to disrupt DNA replication and induce apoptosis. This can be accomplished using compounds that cross-link DNA and compounds that are incorporated into DNA during cell replication by mimicking nucleotides, both of which lead to catastrophic failure during DNA replication, thereby prompting apoptosis. One well known example of a compound that works through physical DNA alteration is cisplatin. Cisplatin was one of the first platinum containing compounds used as an antineoplastic agent for treatment in a variety of cancers, and is part of a standard of care regimen for many different types of malignancies. Cisplatin works by interfering with DNA replication by crosslinking DNA most frequently at guanine residues, resulting in DNA crosslinking. When DNA strand separation fails during the normal course of cell division due to crosslinking, DNA repair mechanisms are called into action that attempt to rectify the failure of separation. Nucleotide excision repair mechanisms can often mitigate intrastrand crosslinking, depending on the particular nature and location of the crosslinking, however, interstrand crosslinks are not repaired by these nucleotide

repair mechanisms. The inability to repair the crosslinks ultimately leads to activation of downstream signaling cascades involving p53, MAPK, and p73 which lead to the induction of apoptosis. Targeting all rapidly-dividing cells is effective at killing cancerously transformed cells, but also targets normal rapidly-dividing cells, leading to the oft-dreaded side effects most commonly associated with chemotherapy, including loss of hair, nails, immunosuppression, and gastrointestinal distress.

A number of targeted therapies exist that attempt to hone in on cancerous cells by targeting particular molecular targets present in cancer cells. Targeted therapies specifically target gene products specific to cancerously transformed cells, such as the targeting of onco-fusion proteins, tyrosine kinase inhibition of growth factors present in mutated forms on the surface of cancer cells, or other gene products specific to cancerously transformed cells. For NSCLC, EGFR is a common target for a targeted therapeutic approach. Therapies that target EGFR work by targeting either EGFR's tyrosine kinase domain or by blocking EGFR's extracellular ligand binding domain. Both approaches ultimately inhibit EGFR signal transduction, thereby working to block cellular proliferation and survival. Tarceva (erlotinib) is one commonly used agent that targets the tyrosine kinase domain inhibitor (EGFR-TKI) for NSCLC treatment. Zactima (vandetanib) is another EGFR-TKI that additionally targets the vascular endothelial growth factor receptor (VEGFR), and has been under investigation for use in treating NSCLC. Targeted therapies are not without side effects of their own, but they can decrease damage done to normal cells in the body, helping to minimize side effects traditionally associated with chemotherapy.

Regardless of the chemotherapeutic approach used, the broad goal is the same: to halt replication of cancer cells. Cell replication is a complex process involving the transmission of signals from outside the cell to the cell surface, initiating cell signaling pathways that lead to the interior of the nucleus and ultimately cell replication, and physical environmental cues can lead to changes in proliferation of cells through communication via cell-cell contacts [63-65]. With this in mind, and considering the changes in proliferation, EMT marker expression, and cell cycle

progression observed in response to cyclic stretch in the previous studies, we wanted to look at the impact of a mechanically active culture environment on cellular responses to chemotherapeutic agents in comparison to responses observed in cells cultured in a static environment.

4.2 Methods

4.2.1 Cell Culture and Mechanical Stimulation

The two non-small cell lung cancer (NSCLC) lines used in this study, a bronchoalveolar line NCI-H358 (ATCC) and an alveolar adenocarcinoma line A549 (ATCC), were obtained from American Type Culture Collection (ATCC). H358 cells were cultured in RPMI-1640 (Sigma Aldrich) and A549 cells were cultured in HAM's F12K (ATCC). Both were supplemented with 10% Fetal Bovine Serum (Sigma Aldrich) and 1% Penicillin Streptomycin (Sigma Aldrich).

Both cell lines were individually cultured in six-well Bioflex Collagen I plates (Flexcell International) as described previously. To compensate for an anti-proliferative effect observed in mechanically stimulated cells in trial studies for this project, a differential seeding density was used for each cell line to achieve an approximately equivalent degree of confluence immediately prior to application of a drug treatment (three days). This was intended to minimize differing amounts of cell-cell interaction between mechanically active or statically cultured cells as a variable. H358 cells were seeded at 100,000 cells/well for static cells and 170,000 cells/well for the group exposed to forces. A549 cells were seeded at 20,000 cells/well for static cells and 35,000 cells/well for cells exposed to forces. Cells were allowed to attach to the plate for 24 hours prior to the application of forces. After 24 hours, a FX-4000 Tension plus unit (Flexcell International) was used to apply a tensile force to cells, as described in Chapter 1.4.

4.2.2 Administration of Chemotherapeutic Agents

Three drugs were investigated for this study: cisplatin, Tarceva (erlotinib), and Zactima (vandetanib). One of three drugs were applied to randomized wells for the "dosed" cell groups for

both mechanically active and static cell culture groups at 72 hours after initial seeding of cells; this was 72 hours after application of tensile forces to the mechanically active cell culture groups. A dose corresponding to the IC_{90} for each drug, chosen to ensure significant inhibition of cell growth in statically cultured cells, was determined using serial dilutions of drug in a dose-response study for each cell line, conducted under standard static culture conditions in a 96-well plate. The calculated IC_{90} values for each were very similar in both cell lines, leading to use of the same drug concentrations for drug dosing in both cell lines for each drug. Each drug was dissolved in DMSO and spiked into cell culture media to produce final concentrations after addition of 1 mL to the cell culture wells as follows: 5 μM for Tarceva, 50 μM for cisplatin, or 50 μM for Zactima (Table 2). The “No Drug” groups for each cell line were given 1 mL of culture media spiked with DMSO only at an amount equivalent to the amount of DMSO used in the drug group. Cells were then cultured for an additional three days, either statically or using the Flexcell as described above corresponding to their original forces or no-forces designation.

4.2.3 Cell Harvesting and Counting

Three days (144 hours total) after administration of drug cells were harvested from each well individually using TrypLE (Gibco) and transferred to new labeled six-well plates in order to maintain treatment group identities. Briefly, media was removed from the culture wells to their corresponding new labeled six-well plates and 300 μL of TrypLE was added to each culture well. Each well’s reserved media was then used to transfer dislodged cells from the culture wells to the new plates. The volume of each well was measured and brought up to a total volume of 4 mL using phosphate-buffered saline. Cell counts were then taken using 1 mL of cells/media from each well using a Vi-CELL Cell Counter (Beckman Coulter) and reported as a cell count per 4 mL of media.

4.2.4 Data Analysis

Viable cell counts as reported by the Vi-CELL are per 1 mL of sample. These reported cell counts were converted to viable cell counts per original sample well volume of 4 mL by multiplying each reported cell count by four. The viable cell counts for each of the three drug studies and each cell type were separated into a “No Forces” group not exposed to a cyclic tensile stretch, and a “With Forces” group that was subjected to cyclic stretch for the duration of exposure to one of the three drugs. Viable cell counts were compared using two-way ANOVA with a Bonferroni post-hoc analysis.

In order to look at how exposure to forces impacts the effect of the drugs used in this study, a percent reduction in viable cell counts for both forces treatment groups was calculated for each cell line and drug combination. The percent reductions observed for the “No Forces” and “With Forces” groups were calculated as follows: the mean viable cell count for each drugged group was subtracted from the mean viable cell count for the corresponding un-drugged group. This difference was then divided by the mean viable cell count for the un-drugged group, yielding a percent reduction. Data was analyzed using a Student’s t-test. Significance was set at $p < 0.05$. All statistical analyses were conducted using GraphPad Prism Version 5.04 (GraphPad Software, Inc.). Each experiment was repeated a minimum of three separate times.

4.3 Results

4.3.1 Zactima Increases Cell Death in Mechanically-Stretched H358 Cells

Significant main effects were seen for drug treatment in both A549 cells ($F(1,4)=22.02$, $p=0.0094$) and H358 cells ($F(1,4)=13.94$, $p=0.0202$), however, though reductions in cell counts were observed with tensile stretch, the main effect of tensile stretch was short of significance in both cell lines. An interaction effect between Zactima and mechanical cell culture was not observed in either cell line. See Figure 13a and Figure 13c for A549 and H358 cell counts, respectively.

Comparing the “No Forces” and “With Forces” groups for A549 treated with Zactima, there was perhaps a slightly greater reduction in the percent reduction in viable cell counts in the “Tensile Stretch” group than in the static culture group at the end of the six-day study, however this was not considered significant (Figure 13b). In H358 cells, a significantly greater percent reduction in viable cell counts in Zactima treated cells exposed to forces was seen at the end of treatment as compared to unstretched cells (Figure 13d).

4.3.2 Tarceva Efficacy Slightly Increased in Mechanically Stretched Cells

A549 (Figure 14a and b) and H358 (Figure 14c and d) cells showed statistically insignificant cell viability changes in the “With Forces” groups as compared to cells grown and treated under static culture conditions with Tarceva exposure.

4.3.3 Cisplatin Efficacy Was Decreased in Mechanically Stretched Cells

A549 cells showed significant main effects for the application of tensile stretch ($F(1, 8)=14.58$, $p=0.0051$), for drug treatment ($F(1,8)=35.74$, $p=0.0003$), and a significant interaction effect ($F(1,8)=12.71$, $p=0.0073$). Post hoc comparison with a Bonferroni correction indicated a change in viable cell counts of undrugged cells between stretched and unstretched conditions that was significant ($t(8)=6.748$, $p<0.001$), but drugged cells did not show a significant change with the application of stretch (Figure 15a). H358 cells showed similar results, with a significant main effect for tensile stretch ($F(1,12)=12.49$, $p=0.0041$), for cisplatin treatment ($F(1,12)=18.73$, $p=0.0010$), and a significant interaction effect ($F(1,12)=7.247$, $p=0.0196$). Significant changes were seen in undrugged viable cell counts between stretched and unstretched cultures ($t(12)=4.403$, $p=0.0052$), as well as a significant change between drugged and undrugged cells without a tensile stretch ($t(12)=4.963$, $p=0.0020$). There was no significant difference between drugged cell counts in stretched and unstretched cells and, interestingly, no significant effect of drug on stretched cell counts (Figure 15c). In both cell lines, the application of tensile stretch itself is decreasing cell

counts significantly, however, exposure to tensile stretch also appears to correlate with observed decreases in cisplatin activity.

Cisplatin yielded decreased percent reductions in the “With Forces” groups for both cell lines, with A549 cells showing statistically significant increased reduction in viable cells in the “With Forces” group compared to the unstretched group, ($t(3)=5.907$, $p=0.0097$) (Figure 15b). Changes in H358 cell viability reductions between stretched and unstretched cells were not statistically significant, but showed a similar trend as with A549 cells ($t(3)=1.802$, $p=0.1694$) (Figure 15d).

4.4 Discussion

Cisplatin’s interference with DNA replication leads to the death of the fastest proliferating cells, making it effective against carcinogenic cells, which typically replicate at a faster rate than non-carcinomic cells *in vivo*. In this experiment, both cell lines used were carcinomic allowing for focus on changes seen with the application of a cyclic stretch in the culture conditions. A greater reduction in viable cells was seen in cells not exposed to stretched culture conditions in both A549 and H358 cells, as compared to cells exposes to cyclic stretch. The differences in percent reduction in viable cells between stretched and non-stretched cells was only observed to be statistically significant in the A549 cell line. Considering cisplatin’s greater efficacy against more rapidly proliferating cells, it may be reasonably explained by the presence of a cyclic stretch causing a decrease in proliferation of cells as compared to non-stretched cells, and so a decreased efficacy against cells exposed to a cyclic stretch. The decreased proliferation observed in the study described in Chapter 2 is consistent with the observed decrease in cisplatin efficacy observed here, though the influence of tensile stretch alone on proliferation makes interpretation of these results more complicated.

Zactima acts against malignantly transformed cells through kinase inhibition of a number of cell receptors, including the epidermal growth factor receptor (EGFR), the vascular endothelial growth factor receptor (VEGFR), and RET-tyrosine kinase. EGFR is a transmembrane receptor

tyrosine kinase that plays a central role in the regulation of cell division and cell death. Activation of EGFR through ligand binding on the cell surface leads to dimerization that activates the tyrosine kinase domain. Tyrosine kinase domain activation leads to autophosphorylation of multiple receptor tyrosine residues which results in the recruitment of adapter proteins that subsequently activate a number of intracellular signaling cascades responsible for gene transcription. This increased gene transcription results in increases in cancer cell proliferation, invasion and metastasis (through stimulation of the RAS-RAF-MAPK pathway), and decreased apoptosis (through activation of the PI3K/AKT pathway and the JAK/STAT pathway). Cancer cells often show abnormalities in EGFR signaling through mutations that lead to a hyperactive form of EGFR, or an overexpression of the wild-type form of the receptor. Similar to EGFR's activity, RET-tyrosine kinase and VEGFR activation also leads to increased proliferation and decreased cell death through RAS-RAF-MAPK and PI3K/AKT pathway activation. RET and VEGFR also show increased expression and activating mutations in cancer-transformed cells. Stopping activity of these cell signaling receptors through tyrosine kinase inhibitors (TKIs) have proven useful against a number of cancers for this reason.

Tarceva utilizes a mechanism of action somewhat similar to that of Zactima: it acts as an EGFR inhibitor also through targeting of the tyrosine kinase domain. Both Tarceva and Zactima showed greater reductions in the percentage of viable cells present in stretched cells; this was the case for both cell lines. Only H358 cells treated with Zactima in the presence of a cyclic stretch showed a statistically significant change. Though Zactima and Tarceva are similar in their mechanisms of action, Tarceva showed no significant differences in efficacy between stretched and unstretched cells in either cell line tested. The differences in efficacy observed between Zactima and Tarceva in both cell lines may point to slightly different mechanisms of action between the two drugs. Zactima is an irreversible EGFR inhibitor, whereas Tarceva works reversibly against this receptor. Considering these results in the context of the EMT marker study

conducted in Chapter 2, it has been reported that EMT does play a role in sensitivity of NSCLC cell lines to EGFR inhibitors, such as Zactima and Tarceva, particularly through shifts in N-cadherin and vimentin expression that favor a mesenchymal phenotype [66, 67]. Differences in Zactima and Tarceva efficacy were not significant in A549 cells in this study, so further conclusions relating to the application of mechanical stimulus to cell culture cannot be drawn at this time, though it does provide a potentially intriguing direction for further study. E-cadherin expression levels have also been tied to a cell's sensitivity to EGFR-TKIs, with increased E-cadherin corresponding with increased sensitivity to these agents [68-70]. In this regard, the increased E-cadherin levels observed in mechanically active H358 cultures in Chapter 2 are consistent with the increased sensitivity of H358 cells to Zactima observed in this drug study. The differences observed between Zactima and Tarceva may be resolved with further study, though it should be noted that AstraZeneca withdrew its new drug application for Zactima as a treatment for NSCLC in late 2009 due to lack of significant improvement in patients with NSCLC.

Looking back at the cell-cycle study conducted in Chapter 3, it is interesting to note the correlation between cell behavior in this cell cycle study and efficacy of drugs related to the application of mechanical stimulation. Cisplatin resistant NSCLC cells have been shown to accumulate in G0/G1 of the cell cycle [71]. This is consistent with the results observed here: both cancer cell lines here showed increases in G0/G1-stage fractions at 72 hours (statistically significant in H358 cells), the time point at which both cell lines were dosed with drug, and both cell lines showed decreased sensitivity to cisplatin (statistically significant in A549 cells).

One potentially important limitation of this study is the presence of activating *KRAS* mutations in both cell lines used. Both H358 and A549 cell lines have been reported to carry activating *KRAS* point mutations in codon 12, a heterozygous c.34G>T/p.Gly12Cys mutation in H358 cells and a homozygous c.34G>A/p.Gly12Ser mutation in A549 cells [72]. Both these mutations have the effect of rendering KRAS constitutively active, allowing KRAS signaling to occur with or without

upstream activation of EGFR, leading to cell-cycle progression in the absence of EGFR activation. As both Tarceva and Zactima work by inhibiting EGFR signaling, their usefulness against tumors harboring *KRAS* mutations can be limited. The presence of *KRAS* activating mutations can be a strong predictor of response to EGFR-TKI therapies such as Tarceva and Zactima [73], though the ability to predict response based on *KRAS* mutation status may depending on the type of tumor. Molecular subtyping of *KRAS*, among other genes, is routine in the treatment of colon cancer [74], however, the role of *KRAS* mutation status in predicting response to EGFR-TKIs is less definitive in NSCLC [75, 76]. It is not entirely surprising that A549 cells, carrying a homozygous activating *KRAS* mutation, may not respond well to Zactima in either treatment group, and showed no significant difference between the stretched and static cell cultures. H358 cells, carrying a heterozygous *KRAS* activating mutation, responded better as compared to A549 cells, and showed increased efficacy in mechanically stretched cells. The presence of a heterozygous *KRAS* mutation in H358 cells, leading to production of some normal (non-constitutively active) KRAS protein in addition to the altered form, may have contributed to its better response when compared to the response in A549 cells, but the impact of an activating *KRAS* mutation cannot definitively explain the response at this time. Despite the lack of definitive link between the presence of an activating *KRAS* mutation and response to EGFR-TKIs in NSCLC, utilizing cell lines that do not harbor mutations in proteins involved in EGFR signaling, in addition to including a non-tumorigenic cell line, such as the NL-20 line used in the cell cycle study described in Chapter 3, would be beneficial in studies of the response of stretched cells to drugs, particularly drugs such as the EGFR-TKIs described here.

There are a few ways that the drug dosing approach itself may be improved in this study, and these could serve as potential starting points for future exploration of this topic. The IC_{90} value, as determined by a dose-response study in both tumorigenic cells lines 96-well plates as described above, was used as the drug dosing concentration for each cell line. This high dose

was chosen to significantly inhibit cell growth in non-stretched cells, however, taking each drug dose down to its IC_{50} value may provide a better view of growth inhibition changes with applied stretch. Another potentially interesting approach to investigating changes in response to chemotherapeutic agents in the presence of mechanical stimulation could involve conducting a dose-response study for each drug in mechanically active cultures versus static cultures to create comparative IC_{50} values.

In conclusion, we demonstrated that *in vitro* exposure of cells to mechanical stimulation can result in altered cellular responses to drug, though explanations for these altered responses still remain to be understood. The differences in biochemical profiles and signaling pathway alterations between these cells lines themselves may contribute to differing responses to the same drug, which underscores some of the continued general difficulties in developing new treatments for cancer. As our understanding of cellular mechanics and mechanotransduction continues to increase, the incorporation of physiologically representative forces to cell culture can allow research and development paradigms for the discovery of new cancer drugs to evolve. Along with development of high-throughput approaches for mechanically active cell culture models, the potential exists to produce a new and advantageous platform for drug discovery and development.

Chapter 5: Conclusions and Future Directions

5.1 Conclusions

In this study we used a dynamic cell culture system to create mechanically active environmental conditions with the hypothesis that tensile (mechanical) forces in lung cancer cells play an important role in determining cellular response to chemotherapeutic agents. In particular, we wanted to compare cells cultured with exposure to a tensile force, and compare those cells to cells cultured under static *in vitro* culture conditions classically used in biological studies.

The first study investigated proliferation changes and changes in expression levels of selected EMT-associated proteins in A549 and H358 cell lines in response to a tensile stretch. Both cell lines showed decreased proliferation with exposure to a tensile stretch over the duration of the study. Observation of the morphological changes showed that H358 cells tended to detach from the wells and form spheroid-like aggregates in the mechanically active culture environment. Shifts in expression levels of selected EMT-associated markers were somewhat consistent with the morphological changes seen, particularly in H358 cells. Further, EMT marker levels in both cell lines hinted toward the epithelial-like H358 cell line showing less signs of EMT, and the more mesenchymal A549 cell line showing more signs of undergoing EMT and a more invasive phenotype. As EMT is a hallmark in metastasis formation, and as EMT has been shown to play a critical role in resistance of cancer to chemotherapies [73], this study serves as an interesting starting point for further investigation of the role of mechanotransduction in the response of cancer cells to drugs and in cancer drug discovery.

The second study looked at changes in cell cycle progression in A549 and H358 cells, as well as a non-tumorigenic cell line NL-20, under mechanically active culture conditions at both a 72-hour time point and a 144-hour time point. In mechanically active culture at the 72-hour time point, H358 cells showed an increase in G0/G1 phase cells and a decrease in G2 phase cells,

and this corresponded with increased CDK1, cyclin B1, and p21 expression observed at this time point. A549 cells showed similar increased in CDK1, cyclin B1, and p21 expression in mechanically active cell cultures at the 72-hour time point, but showed an increase only in the number of cells in M-phase; the number of cells in G0/G1, S, and G2 were comparable in both active and static cell cultures. H358 cells at the 120-hour time point showed a decrease in S-phase cells and an increase in M-phase cells in mechanically active cultures, corresponding with the observation of increased p21 levels in these cells. The A549 cell line showed decreases in both G0/G1 and S phase cells at 144 hours in mechanically active cultures. This was coupled with observed decreases in cellular levels of p21, cyclin B1, and CDK1 at this time point.

The third study compared cellular responses of two different cell lines to three different chemotherapy drugs in with or without exposure to mechanically active culture conditions. For cells exposed to cisplatin, the A549 cell line showed decreased efficacy in cells cultured in a mechanically active environment. For Zactima-treated cells, the H358 cell line showed increased reduction in viable cells in the mechanically active growth environment.

Taken together, we showed a decreased efficacy of cisplatin in cells grown with tensile stretch, corresponding with observed increases in G0/G1 cell cycle fractions at the time of drug dosing (72 hours) due to stretch alone. We also showed an increased efficacy of EGFR-TKIs in the bronchoalveolar H358 cell line, which corresponded with increased E-cadherin expression in stretched cells; the changed efficacy of EGFR-TKIs observed appeared to be influenced, in part, by EMT marker expression alterations in stretched cells. The presence of a strong anti-proliferative effect in both cell lines with tensile stretch alone as well as the presence of activating *KRAS* mutations complicates interpretation of the drug study results, however future study could assist in disentangling the response to stretch from the response to drug.

5.2 Future Directions

As our understanding of the pathways involved in and influenced by mechanotransduction increases, the incorporation of physiologically relevant mechanical stimulation in cellular research paradigms will almost certainly become not only necessary but also routine. The incorporation of mechanotransduction in cell culture has important implications for both our understanding of cellular processes in our bodies and for the development of new treatments for when these cellular processes go awry. Though interest in studies involving the impact of mechanically active cell culture on cellular behavior has increased over the past several years, this field is still relatively new and many opportunities for discovery still remain. Numerous directions for future work in mechanotransduction and cell culture are available in the context of the studies described in this thesis; a few possibilities are described below.

5.2.1 High Throughput Cell Culture Format

In this study, the bioreactor used was a commercially available model from Flexcell International Corporation that was available in a six-well format. The adoption of a cell culture model such as the one used in this study would require development of a high-throughput format for such a model to be of practical use in a typical laboratory setting, but particularly for use in any drug discovery applications, the potential for which this study was intended to investigate. For practical reasons, the process of drug discovery and development requires a culture format that allows for the screening of numerous drug candidates simultaneously to detect leads for subsequent study. It is simply not feasible for the purposes of screening numerous drug candidates to rely on a six-well cell culture format, and other studies of biological effects of mechanically active culture conditions, such as those in the studies presented here, would benefit tremendously from the availability of a greater number of sample wells. Flexcell International has developed a version of the culture plates used in this study that are scaled down to a 24-well format, but such plates still represent a prohibitively low-throughput format for routine use in

research and development applications. A variety of new bioreactors have been developed and investigated to bring a higher-throughput format [77], which will certainly continue to bring the study of the mechanics of cellular life into greater prevalence.

5.2.2 Proteomics

During the course of this study western blotting was used to probe for relative changes in abundance of a very small number of proteins related to cell cycle progress. Looking at cellular protein abundance changes on a total cell scale has the potential to point to differences in protein abundance that otherwise may not have immediately followed from the results presented in the studies that serve as the focus of this paper.

Proteomic studies have been used as a broad-scale approach to the identification of proteins of interest in mechanically active cultures of varying types, including human optic nerve head astrocytes [78] and rat proximal tubule cells [79], to list a very few. Frequently, whole cell lysates are created and separated first by isoelectric focusing (IEF), in which proteins are separated on a gradient pH strip by differences in their isoelectric points. Strips containing IEF-focused proteins are then separated by weight using SDS-PAGE electrophoresis. The result is a gel that represents a grid of proteins for the separated sample, and protein grids can then be compared computationally to detect differences in protein expression for subsequent downstream mass-spectrometric identification. Such a broad-scale approach would be potentially interesting to probe for differences in cellular proteomes of cells cultured under the mechanically active conditions studied here.

5.2.3 Incorporation of Representative Extracellular Environment

The cell culture conditions under investigation in this study involved the addition of equibiaxial strain to cells growing in monolayers in culture wells. Culturing cells in monolayers *in vitro* has been and will continue to be an important approach for biological studies, however, cells cultured in monolayers in traditional culture plates are not exposed to the variety of mechanical and

chemical signals experienced when cultured in more complex three-dimensional structures. Cells in the body reside in a complex three-dimensional network of extracellular matrix proteins, polysaccharides and proteoglycans, as well as other types of cells, that all serve to provide structural and chemical support to the groups of cells comprising various tissues. The incorporation of a more representative cellular environment, one that more closely represents the *in vivo* environment through incorporation of co-culture models, three dimensional culture environments, and inclusion of a more representative combination of extracellular matrix components could go far toward understanding the impact of mechanotransduction in the context of a cell's multifaceted *in vivo* environment.

Figures and Tables

Figures

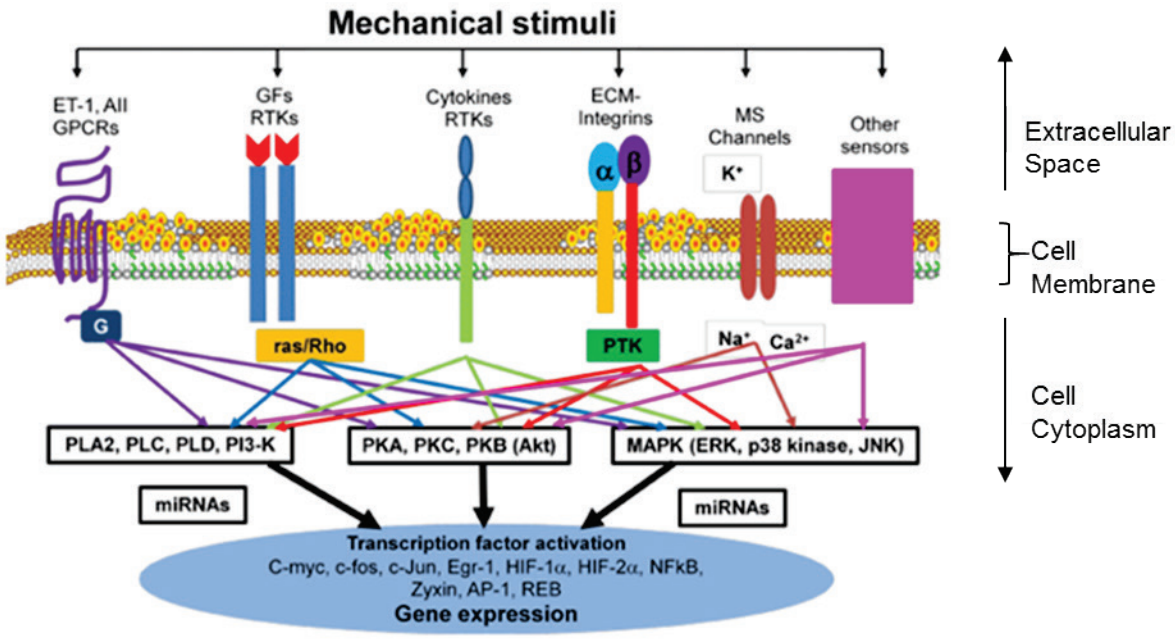

***Figure 1**: **General schematic depicting some examples of cellular mechanotransduction**. Mechanical stimuli external to the cell activate cell-surface mechanical sensors in the plasma membrane which convert physical stimuli into biochemical signals. These signals result in the activation of various cellular signaling pathways, leading to the regulation of gene expression and, ultimately, the modulation of cellular function. Adapted from Huang et al. [80].*

(a) – Flexcell Base station

(b) – Bioflex plate

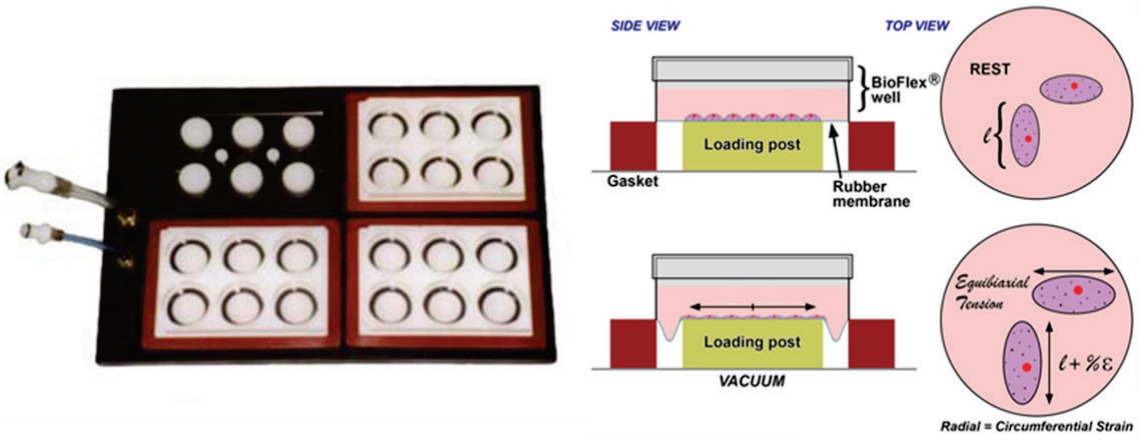

Figure 2: Flexcell base station and Bioflex plate*. The base station holds four flexible-well plates that are distensible from below via connection to vacuum pressure through the tubing shown on the left of the base station (a). Vacuum pressure pulls the flexible wells of the Bioflex plate down over a loading post, delivering equibiaxial tension to cells cultured in the plate (b).*

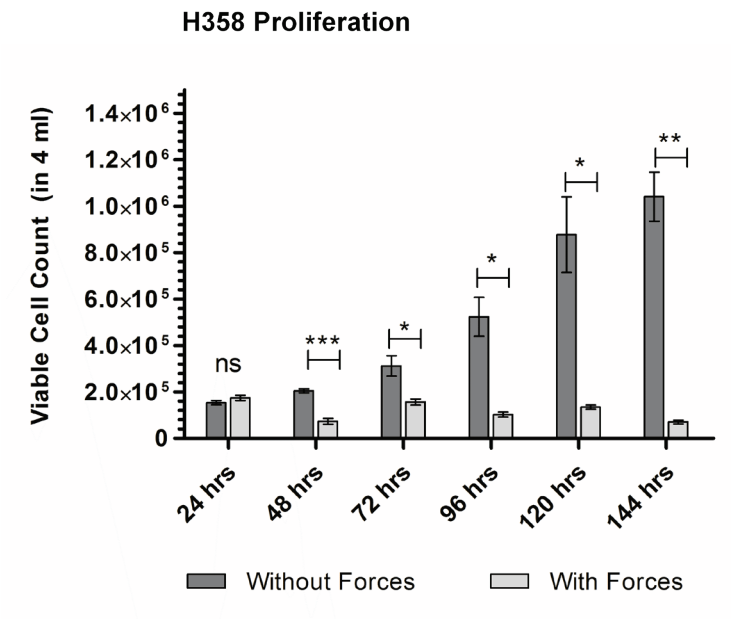

Figure 3: H358 bronchoalveolar epithelial cells show a halt in proliferation with mechanical cell culture conditions*. Each time point indicates the time elapsed from initiation of the experiment. Cells were allowed to grow statically in both groups for 24 hours; the application of a tensile stretch to the "With Forces" group occurred immediately following cell counts for the 24-hour period. The potential impact of applied tensile stretch is present starting at the 48-hour time point and beyond. Significant differences in viable cell counts between actively at statically cultured cells at each time point appeared at 48 hours (t(3)=15.06, p=0.0006), and continued at 72 hours (t(2)=5.912, p=0.0274), at 96 hours (t(2)=8.621, p=0.0132), at 120 hours (t(2)=7.898, p=0.0157), and at 144 hours (t(2)=15.83, p=0.0040). Unpaired Welch's t-test was used for comparison of viable cell counts at each time point. Data is shown as mean ± SD.*

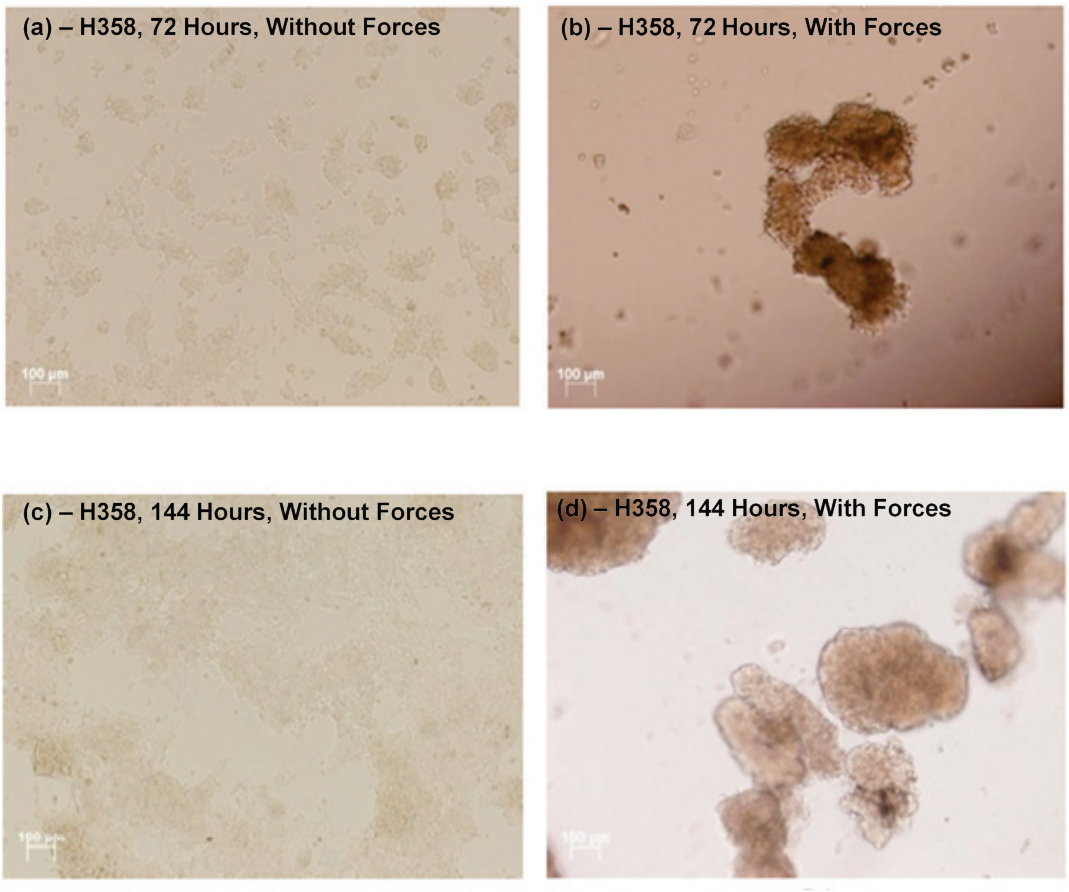

Figure 4: H358 bronchoalveolar cells formed detached spheroidal aggregates with mechanically active cell culture conditions. *Cells cultured without mechanical stimulation remained adherent to the surface of the wells at 72 hours (a), whereas detachment and clustering of cells is present in cells cultures with mechanical stimulation (b). This is continued at the 144-hour time point, with cells cultured without stimulation remaining adherent (c), and cells cultured with stimulation continuing to show detachment and clustering (d). Scale bar in bottom left of each panel represents 100 μm.*

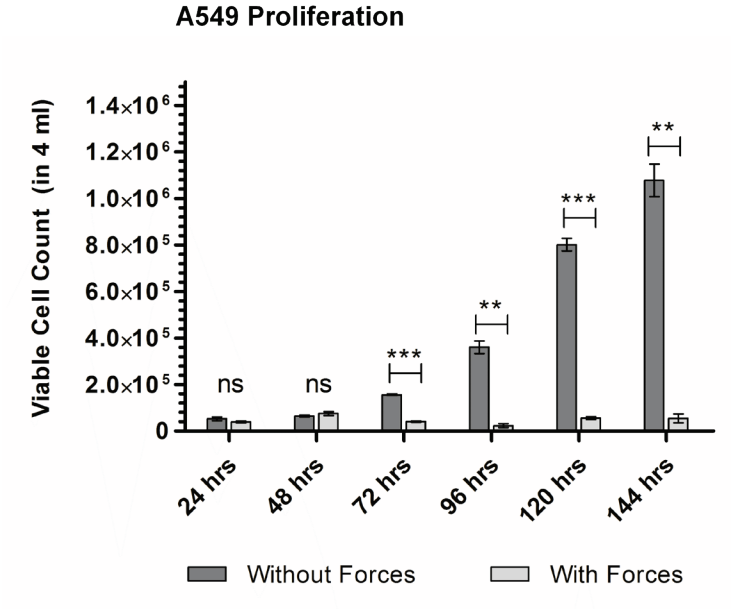

Figure 5: A549 alveolar epithelial viable cell counts exhibit a proliferative halt with mechanical forces*. Each time point indicates the time elapsed from initiation of the experiment. Cells were allowed to grow statically in both groups for 24 hours; the application of a tensile stretch to the "With Forces" group occurred immediately following cell counts for the 24-hour period. The potential impact of applied tensile stretch is present starting at the 48-hour time point and beyond. Significant differences in viable cell counts between actively at statically cultured cells at each time point appeared at 72 hours ($t(3)=46.79$, $p<0.0001$), at 96 hours ($t(2)=20.98$, $p=0.0023$), at 120 hours ($t(2)=46.30$, $p=0.0005$), and at 144 hours ($t(2)=24.36$, $p=0.0017$). Unpaired Welch's t-test was used for comparison of viable cell counts at each time point. Data is shown as mean ± SD.*

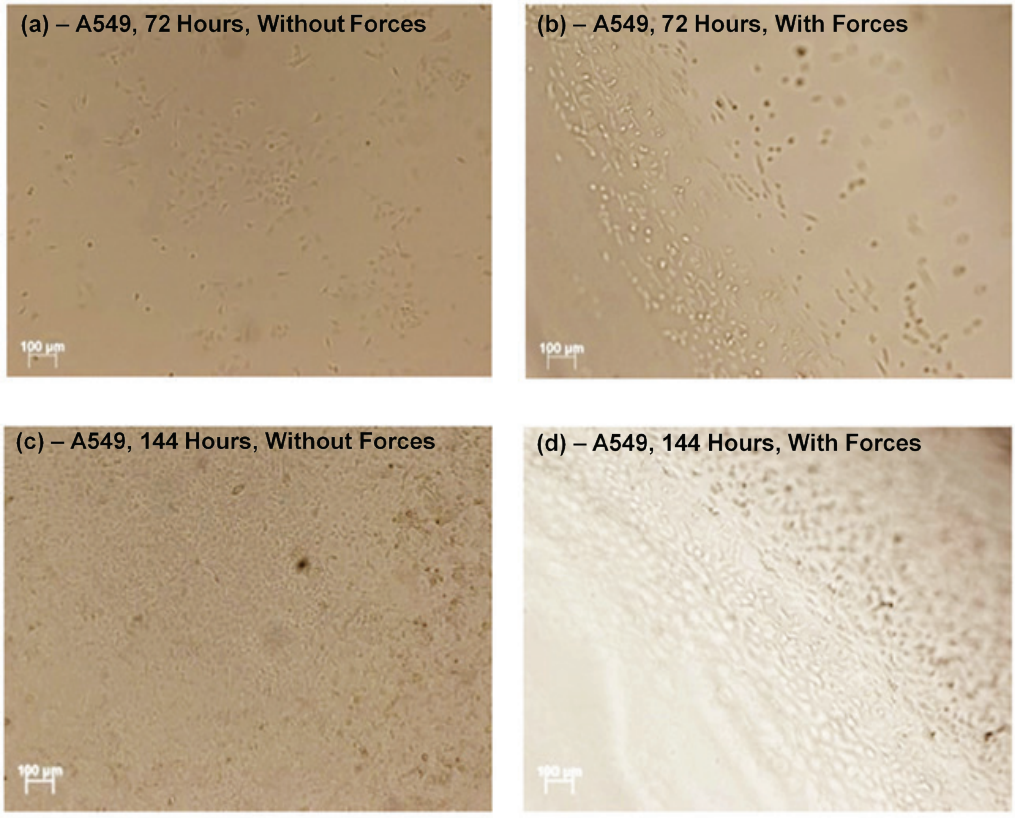

Figure 6: A549 cells remained adherent and morphologically unchanged for the duration of the experiment, with or without exposure to mechanically active culture conditions. *At 72 hours, both the statically cultured group (a) and the mechanically active cultured group (b) remained adherent. This is continued at the 144-hour time point for statically cultured cells (c) and the mechanically active group (d). Scale bar in each panel represents 100 µm.*

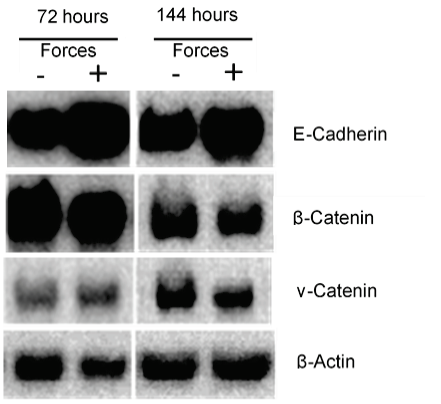

(a)–H358 Epithelial Marker Expression, 72 hours and 144 Hours

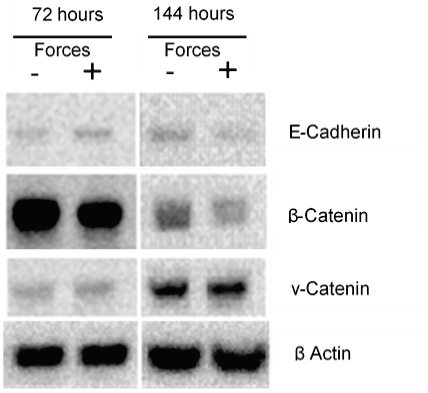

(b)–A549 Epithelial Marker Expression, 72 hours and 144 Hours

Figure 7: Expression of the epithelial marker E-cadherin is increased in H358 bronchoalveolar epithelial cells at 144 hours of culture with forces. *Comparison of relative epithelial marker levels between static and active culture in H358 (a) and A549 (b) cells. H358 cells showed increased E-cadherin at 144 hours with forces (a). Relative expression of β-catenin was slightly lower in A549 cells at the 144-hour time point (b). All other markers were relatively unchanged.*

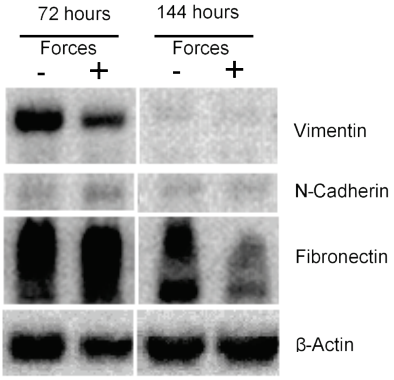

(a)–H358 Mesenchymal Marker Expression, 72 hours and 144 Hours

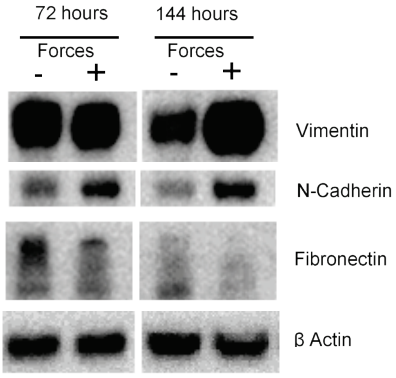

(b)–A549 Mesenchymal Marker Expression, 72 hours and 144 Hours

Figure 8: Mesenchymal markers are decreased in H358 bronchoalveolar cells and increased in A549 alveolar cells. *H358 cells showed decreased Vimentin expression at 72 hours, and decreased Fibronectin levels at 144 hours (a). A549 showed increases in Vimentin at 144 hours and N-cadherin at both time points (b). All other markers were relatively unchanged.*

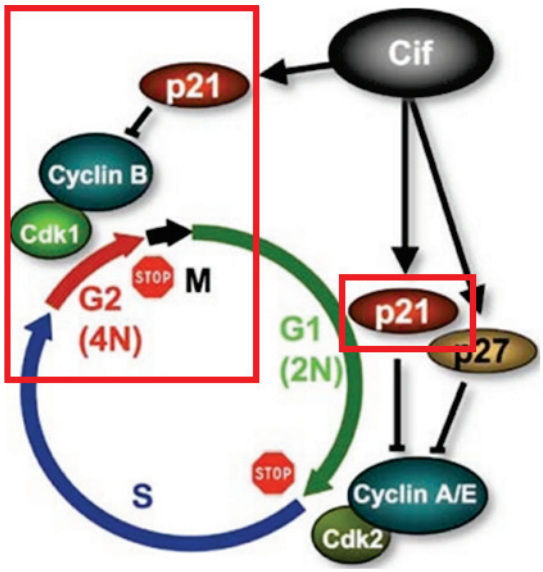

Figure 9: Generalized depiction of cell cycle proteins and checkpoints investigated. *The progression of cells through the distinct phases of the cell cycle is monitored through activity of cell cycle associated proteins. Cyclin B1-cdk1 complexes play a role in successful G2/M transition. P21 plays an inhibitory role both through blockade of cyclin B1-cdk1 activity at the G2/M transition point as well as through inhibition of G1/S transition. Cell cycle checkpoint proteins investigated in this study are marked in red. Adapted from Taieb et al. [66].*

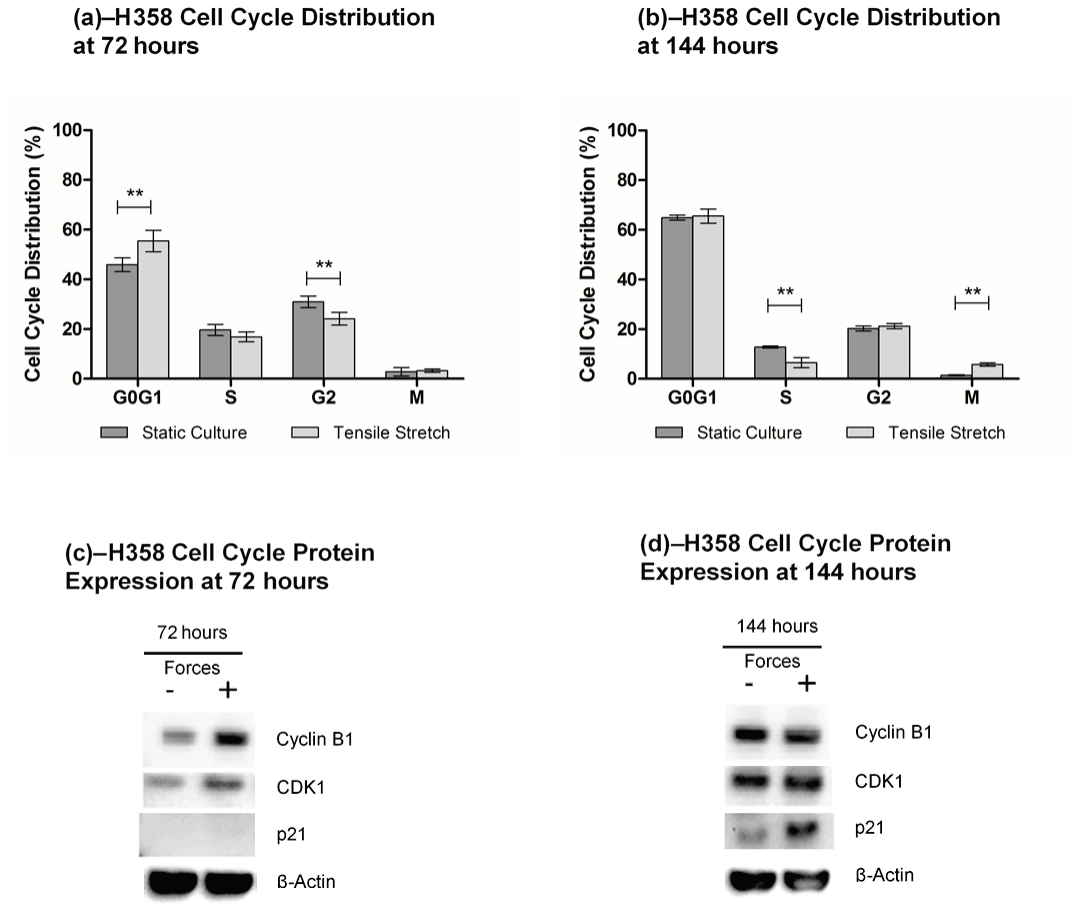

Figure 10: Bronchoalveolar epithelial H358 cells show increased G0/G1 cell fractions at 72 hours, with a shift to increased mitotic-phase cells at 144 hours. *After 72 hours, the percentage of cells in G0/G1 was increased in cells culture with exposure to a cyclic stretch ($t(8)=4.186$, $p=0.0031$) and the percentage of G2 cells was decreased in the mechanically active culture environment ($t(8)=4.437$, $p=0.0022$) relative to static culture (panel a). This corresponded with increased levels of Cyclin B1 at 72 hours in the active culture environment (panel c). At 144 hours decreased S-phase ($t(4)=5.358$, $p=0.0059$) and increased M-phase ($t(4)=10.68$, $p=0.0004$) cell fractions were observed in cells grown with tensile stretch (panel b), corresponding with increased p21 (panel d). Unpaired Student's t-test was used for comparison of cell cycle distribution at each cell cycle stage. Data in panels (a) and (b) are shown as mean ± SD.*

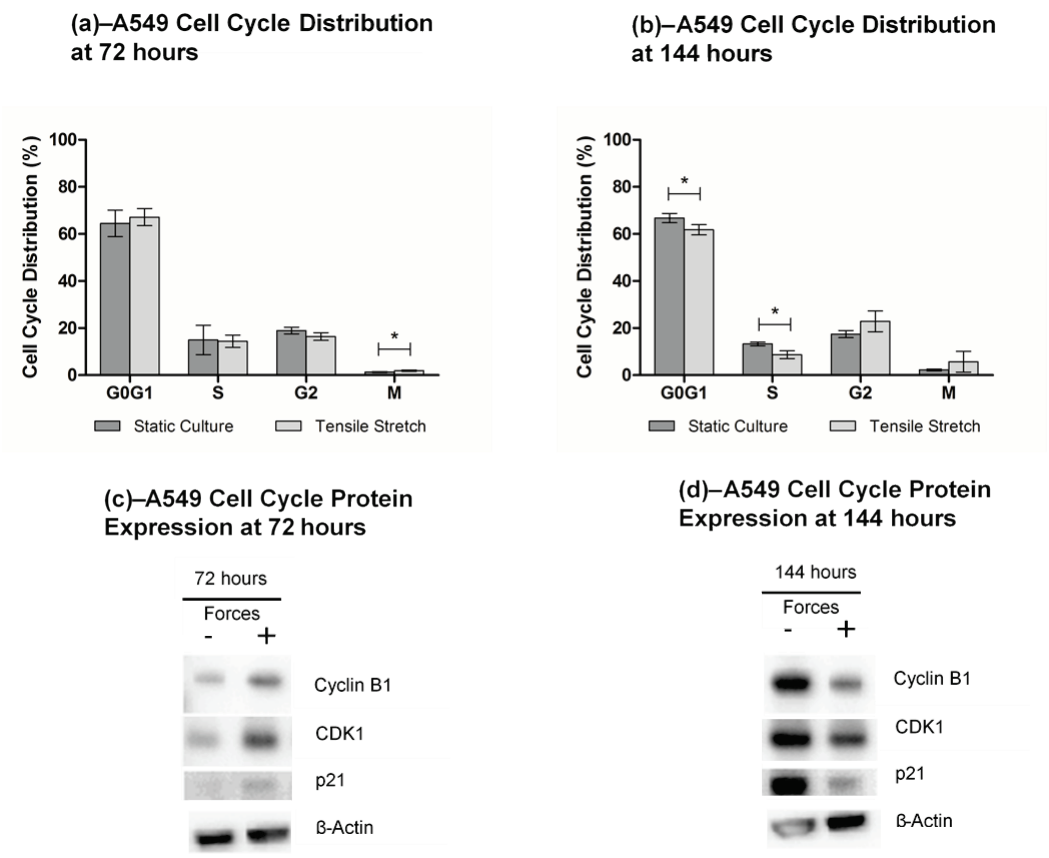

Figure 11: Shorter-term exposure to mechanically active culture yields slight but significant increases in mitotic A549 alveolar epithelial cells. *Distribution of A549 cells in cell cycle phases and protein expression after 72 hours of culture (a and c, respectively) or 144 hours of culture (b and d, respectively). The percentage of cells in M-phase after 72 hours of culture was increased in cells cultured with cyclic stretch ($t(4)=2.950$, $p=0.0420$) (panel a), corresponding to increased Cyclin B1, CDK1, and p21 (panel c). After 144 hours, cells culture with cyclic stretch showed decreases in both G0/G1 ($t(4)=2.962$, $p=0.0415$) and S-phase ($t(4)=4.273$, $p=0.0129$) distributions (panel b), accompanying decreased relative amounts of Cyclin B1, CDK1, and p21 (panel d). Unpaired Student's t-test was used for comparison between statically cultured cells cultured with tensile stretch of cell cycle distribution for each phase. Unpaired Student's t-test was used for comparison of cell cycle distribution at each cell cycle stage. Data in panels (a) and (b) are shown as mean ± SD.*

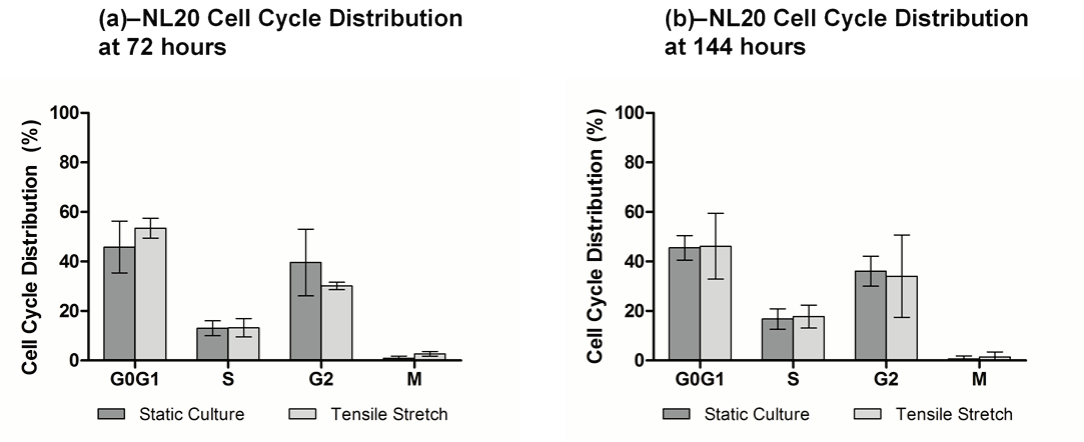

Figure 12: Non-tumorigenic lung NL-20 epithelial cells show no differences in cell cycle distribution with forces. *Distribution of NL-20 cells in cell cycle phases after 72 hours of culture (a) or 144 hours of culture (b). No significant differences were seen between cells cultured statically versus cells cultured with cyclic stretch at either time point. Unpaired Student's t-test was used for comparison of cell cycle distribution at each cell cycle stage. Data in panels (a) and (b) is shown as mean ± SD.*

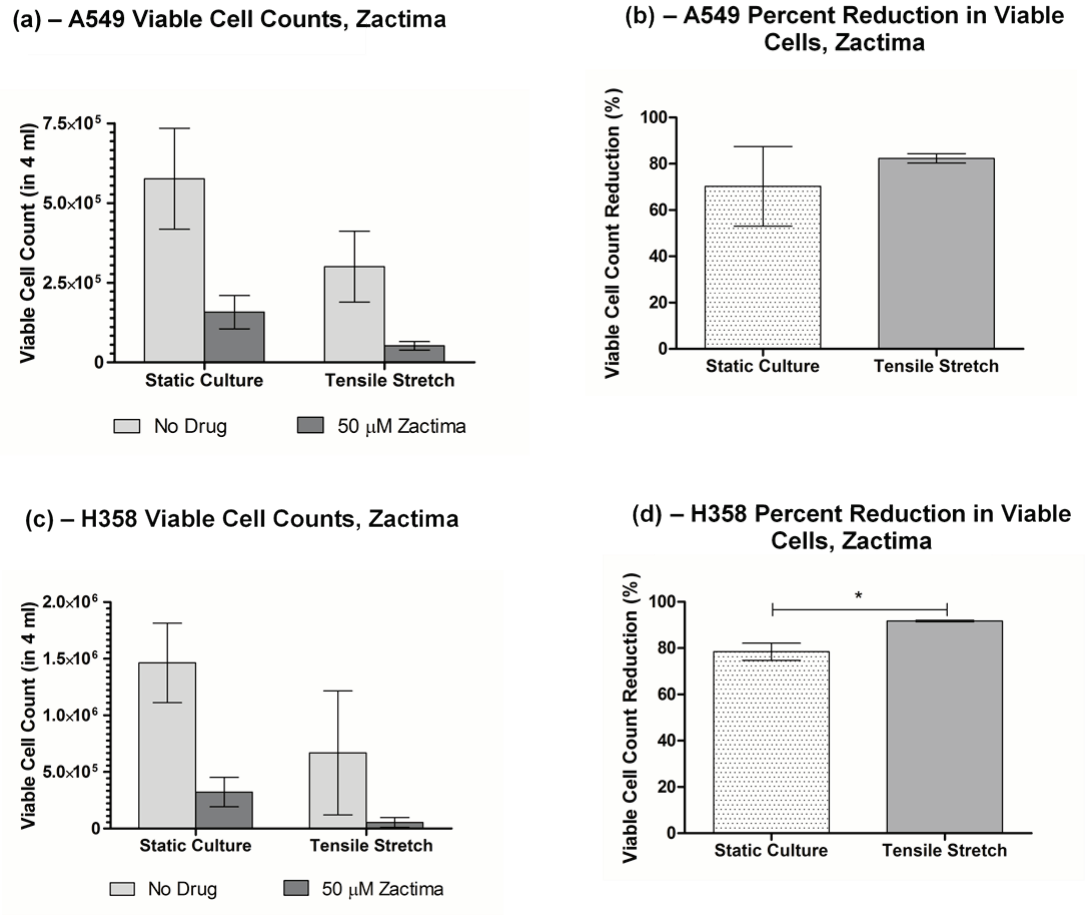

Figure 13: Zactima shows increased efficacy against H358 bronchoalveolar epithelial cells when applied to mechanically active culture. *Viable cell counts for A549 alveolar cells (a) and H358 bronchoalveolar cells (c) show decreases in viable cell counts with the application of a cyclic stretch to cell culture. The percent reduction increased in both cell lines (b and d), but was only significant in H358 cells (d) ($t(2)=5.030$, $p=0.0373$). Viable cell counts were compared using two-way ANOVA with Bonferroni post hoc multiple comparisons. Unpaired Student's t-test was used for percent reduction comparisons. Data is shown as mean ± SD.*

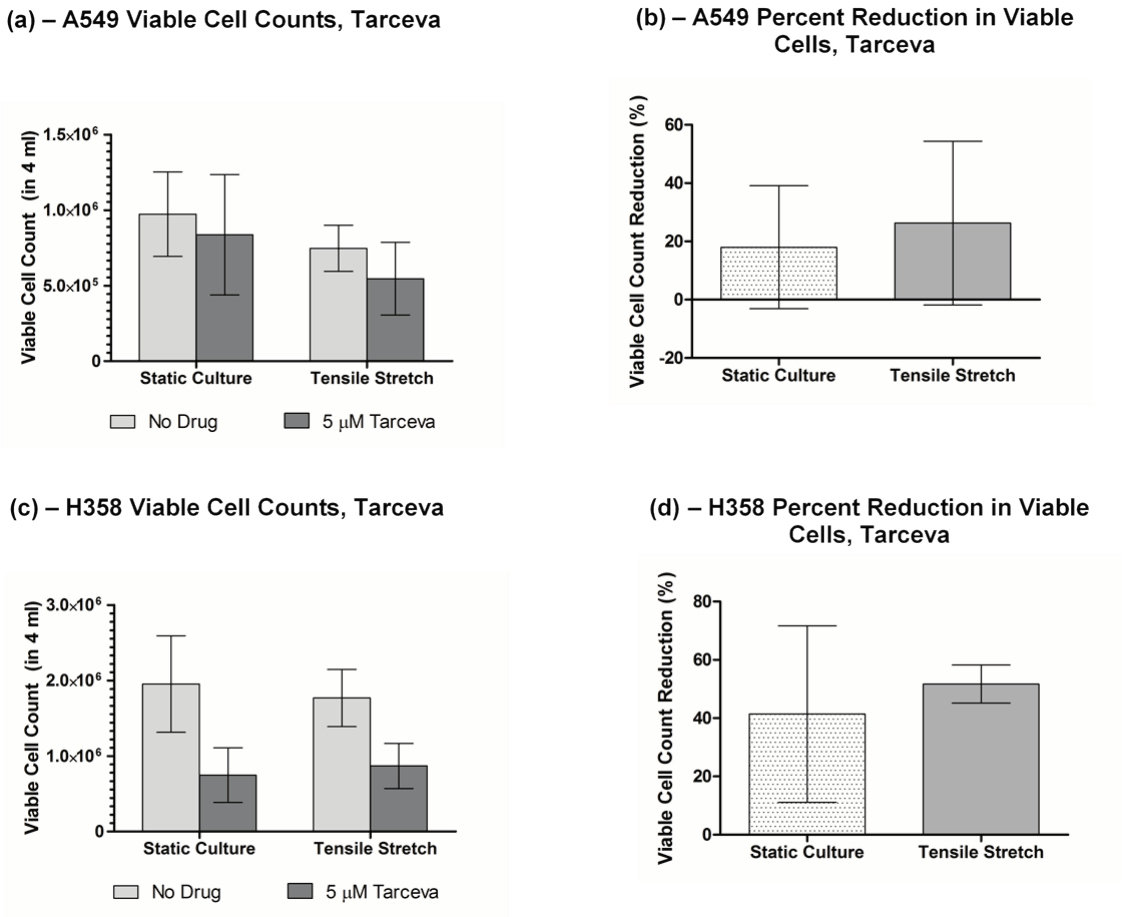

Figure 14: Mechanically active culture had no significant effect on Tarceva efficacy. *Viable cell counts in A549 (a) and H358 (c) cells. The percent reduction was slightly but statistically insignificantly higher in both cell lines when cultured in mechanically active wells (b and d). Viable cell counts were compared using two-way ANOVA with Bonferroni post hoc multiple comparisons. Unpaired Student's t-test was used for percent reduction comparisons. Data is shown as mean ± SD.*

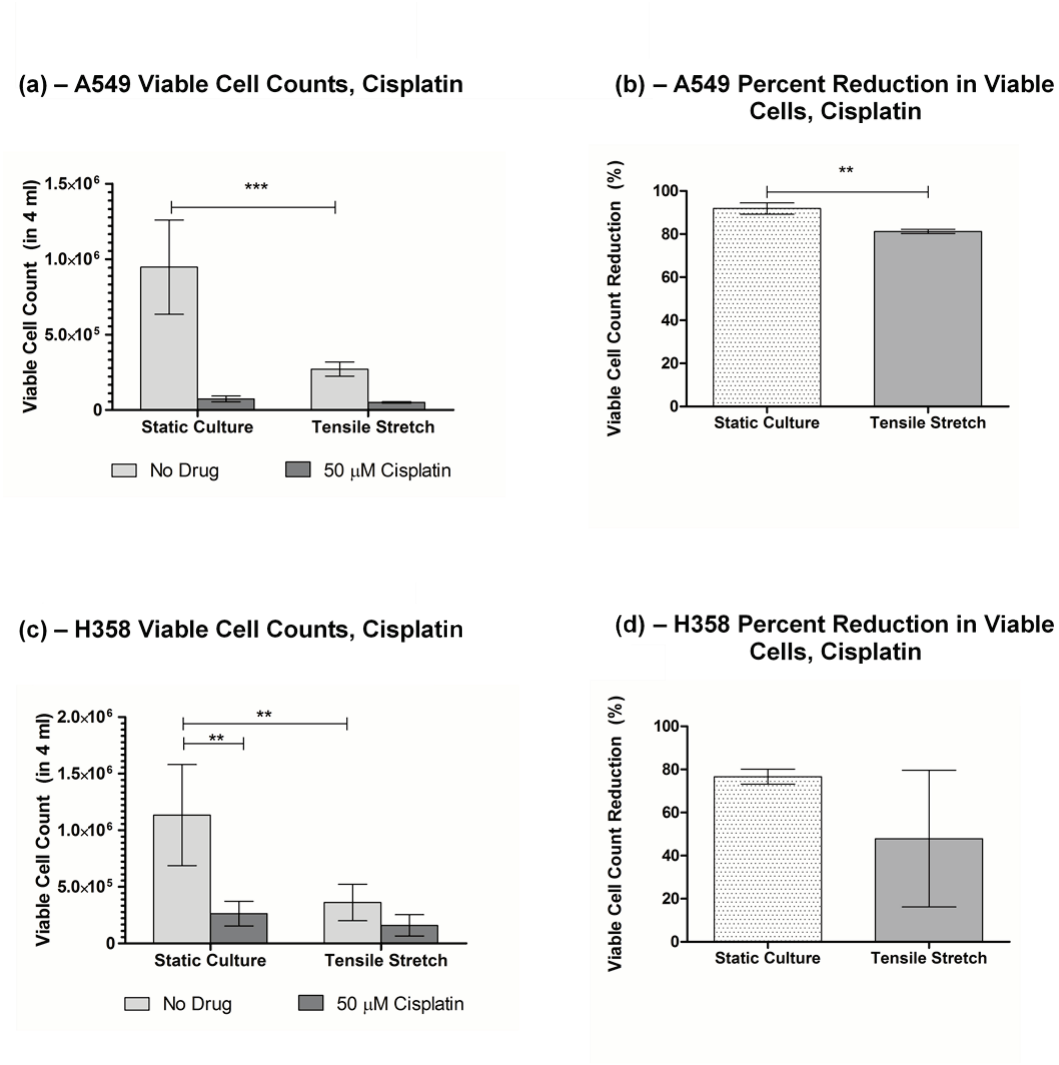

Figure 15: Cisplatin shows decreased efficacy against A549 alveolar epithelial cells when applied to mechanically active culture. *Viable cell counts for A549 alveolar cells and H358 bronchoalveolar cells show decreases in viable cell counts with the co-application of a cyclic tensile stretch and 50 μM cisplatin to cell culture (panels a and c, respectively). Viable cell counts were not significantly different in between cells cultured statically and cells cultured with tensile stretch in drugged cells, but that undrugged cells did show significant differences between stretched and unstretched cells ($t(8)=6.748$, $p<0.001$) (a). The percent reduction decreased in both cell lines (b and d), but was only significant in A549 cells (b) ($t(3)=5.907$, $p=0.0097$). Viable cell counts were compared using two-way ANOVA with Bonferroni post hoc multiple comparisons. Unpaired Student's t-test was used for percent reduction comparisons. Data is shown as mean ± SD.*

Tables

Table 1: *Distribution of cells in each cell cycle phase. The percent fraction of cells in each phase is represented as the mean ± SD.*

		72 hours, *Static Culture*	72 hours, *Cyclic Stretch*	144 hours, *Static Culture*	144 hours, *Cyclic Stretch*
H358		N=5		N=3	
	G0/G1	45.900 ± 2.743	55.440 ± 4.295	64.900 ± 1.054	65.500 ± 2.893
	S	19.700 ± 2.207	16.880 ± 2.036	12.800 ± 0.400	6.533 ± 1.986
	G2	30.960 ± 2.313	24.160 ± 2.529	21.767 ± 1.168	21.233 ± 1.060
	M	2.860 ± 1.701	3.280 ± 0.661	1.467 ± 0.208	5.767 ± 0.666
A549		N=3		N=3	
	G0/G1	64.480 ± 5.631	67.150 ± 3.627	66.767 ± 1.976	61.767 ± 2.155
	S	14.993 ± 6.256	14.367 ± 2.614	13.267 ± 0.777	8.733 ± 1.665
	G2	18.977 ± 1.401	16.417 ± 1.604	17.467 ± 1.528	22.867 ± 4.409
	M	1.333 ± 0.186	1.930 ± 0.297	2.267 ± 0.379	5.700 ± 4.440
NL20		N=3		N=5	
	G0/G1	45.833 ± 10.483	53.467 ± 3.9810	45.520 ± 4.956	46.160 ± 13.306
	S	13.033 ± 3.027	13.233 ± 3.722	16.780 ± 4.117	17.760 ± 4.605
	G2	39.600 ± 13.438	30.100 ± 1.510	36.100 ± 6.026	34.060 ± 16.612
	M	0.933 ± 0.839	2.700 ± 0.917	0.700 ± 1.192	1.440 ± 1.979

Table 2: *List of drugs used in this study, their mechanism of action, and their tested concentration.*

Drug	***Mechanism of Action***	***Tested Concentration (IC_{90})***
Zactima (vandetanib)	Irreversible tyrosine kinase inhibitor (VEGFR and EGFR)	50 μM
Tarceva (erlotinib)	Reversible tyrosine kinase inhibitor (EGFR)	5 μM
Cisplatin	Cross-links DNA to induce apoptosis	50 μM

References

1. Siegel, R.L., K.D. Miller, and A. Jemal, *Cancer statistics, 2016.* CA: A Cancer Journal for Clinicians, 2016. **66**(1): p. 7-30.
2. Nawaz, K. and R.M. Webster, *The non-small-cell lung cancer drug market.* Nat Rev Drug Discov, 2016. **15**(4): p. 229-230.
3. Mak, I.W.Y., N. Evaniew, and M. Ghert, *Lost in translation: animal models and clinical trials in cancer treatment.* American Journal of Translational Research, 2014. **6**(2): p. 114-118.
4. Caponigro, G. and W.R. Sellers, *Advances in the preclinical testing of cancer therapeutic hypotheses.* Nat Rev Drug Discov, 2011. **10**(3): p. 179-187.
5. Bowes, J., et al., *Reducing safety-related drug attrition: the use of in vitro pharmacological profiling.* Nat Rev Drug Discov, 2012. **11**(12): p. 909-922.
6. Hickman, J.A., et al., *Three-dimensional models of cancer for pharmacology and cancer cell biology: capturing tumor complexity in vitro/ex vivo.* Biotechnol J, 2014. **9**(9): p. 1115-28.
7. Jaalouk, D.E. and J. Lammerding, *Mechanotransduction gone awry.* Nature Reviews Molecular Cell Biology, 2009. **10**(1): p. 63-73.
8. Maloney, J.E., et al., *MODIFICATION OF RESPIRATORY CENTER OUTPUT IN UNANESTHETIZED FETAL SHEEP INUTERO.* Journal of Applied Physiology, 1975. **39**(4): p. 552-558.
9. Fewell, J.E., et al., *EFFECT OF TRACHEOSTOMY ON LUNG DEVELOPMENT IN FETAL LAMBS.* Journal of Applied Physiology, 1983. **55**(4): p. 1103-1108.
10. Alcorn, D., et al., *MORPHOLOGICAL EFFECTS OF CHRONIC TRACHEAL LIGATION AND DRAINAGE IN FETAL LAMB LUNG.* Journal of Anatomy, 1977. **123**(JUL): p. 649-660.
11. Moessinger, A.C., et al., *ROLE OF LUNG FLUID VOLUME IN GROWTH AND MATURATION OF THE FETAL SHEEP LUNG.* Journal of Clinical Investigation, 1990. **86**(4): p. 1270-1277.
12. Delorimi.Aa, D.F. Tierney, and H.R. Parker, *HYPOPLASTIC LUNGS IN FETAL LAMBS WITH SURGICALLY PRODUCED CONGENITAL DIAPHRAGMATIC HERNIA.* Surgery, 1967. **62**(1): p. 12-&.
13. Pringle, K.C., et al., *CREATION AND REPAIR OF DIAPHRAGMATIC-HERNIA IN THE FETAL LAMB - LUNG DEVELOPMENT AND MORPHOLOGY.* Journal of Pediatric Surgery, 1984. **19**(2): p. 131-140.
14. Alcorn, D., et al., *MORPHOLOGICAL EFFECTS OF CHRONIC BILATERAL PHRENECTOMY OR VAGOTOMY IN THE FETAL LAMB LUNG.* Journal of Anatomy, 1980. **130**(JUN): p. 683-695.
15. Fewell, J.E., C.C. Lee, and J.A. Kitterman, *EFFECTS OF PHRENIC-NERVE SECTION ON THE RESPIRATORY SYSTEM OF FETAL LAMBS.* Journal of Applied Physiology, 1981. **51**(2): p. 293-297.
16. Wigglesworth, J.S. and R. Desai, *EFFECTS ON LUNG GROWTH OF CERVICAL CORD SECTION IN THE RABBIT FETUS.* Early Human Development, 1979. **3**(1): p. 51-65.
17. Tschumperlin, D.J., J. Oswari, and S.S. Margulies, *Deformation-induced injury of alveolar epithelial cells - Effect of frequency, duration, and amplitude.* American Journal of Respiratory and Critical Care Medicine, 2000. **162**(2): p. 357-362.
18. McAdams, R.M., et al., *Cyclic stretch attenuates effects of hyperoxia on cell proliferation and viability in human alveolar epithelial cells.* American Journal of Physiology-Lung Cellular and Molecular Physiology, 2006. **291**(2): p. L166-L174.
19. Kato, T., et al., *Up-regulation of COX2 expression by uni-axial cyclic stretch in human lung fibroblast cells.* Biochemical and Biophysical Research Communications, 1998. **244**(3): p. 615-619.
20. Mijailovich, S.M., et al., *DYNAMIC MODULI OF RABBIT LUNG-TISSUE AND PIGEON LIGAMENTUM PROPATAGIALE UNDERGOING UNIAXIAL CYCLIC LOADING.* Journal of Applied Physiology, 1994. **76**(2): p. 773-782.
21. Hu, X.B., et al., *Mechanical stress upregulates intercellular adhesion molecule-1 in pulmonary epithelial cells.* Respiration, 2008. **76**(3): p. 344-350.
22. Banes, A., et al., *A new vacuum-operated stress-providing instrument that applies static or variable duration cyclic tension or compression to cells in vitro.* J Cell Sci, 1985. **75**(1): p. 35-42.

23. Dassow, C., et al., *Biaxial distension of precision-cut lung slices.* Journal of Applied Physiology, 2010. **108**(3): p. 713-721.
24. Gorfien, S.F., et al., *EFFECTS OF BIAXIAL DEFORMATION ON PULMONARY-ARTERY ENDOTHELIAL-CELLS.* Journal of Cellular Physiology, 1989. **139**(3): p. 492-500.
25. Williams, J.L., J.H. Chen, and D.M. Belloli, *STRAIN FIELDS ON CELL STRESSING DEVICES EMPLOYING CLAMPED CIRCULAR ELASTIC DIAPHRAGMS AS SUBSTRATES.* Journal of Biomechanical Engineering-Transactions of the Asme, 1992. **114**(3): p. 377-384.
26. Brighton, C.T., et al., *THE PROLIFERATIVE AND SYNTHETIC RESPONSE OF ISOLATED CALVARIAL BONE-CELLS OF RATS TO CYCLIC BIAXIAL MECHANICAL STRAIN.* Journal of Bone and Joint Surgery-American Volume, 1991. **73A**(3): p. 320-331.
27. Ursekar, C.P., et al., *Design and Construction of an Equibiaxial Cell Stretching System That Is Improved for Biochemical Analysis.* PLoS ONE, 2014. **9**(3): p. e90665.
28. Vandenburgh, H.H., *A COMPUTERIZED MECHANICAL CELL STIMULATOR FOR TISSUE-CULTURE - EFFECTS ON SKELETAL-MUSCLE ORGANOGENESIS.* In Vitro Cellular & Developmental Biology, 1988. **24**(7): p. 609-619.
29. Sanchez-Esteban, J., et al., *Mechanical stretch promotes alveolar epithelial type II cell differentiation.* Journal of Applied Physiology, 2001. **91**(2): p. 589-595.
30. Sanchez-Esteban, J., et al., *Mechanical stretch induces fetal type II cell differentiation via an epidermal growth factor receptor-extracellular-regulated protein kinase signaling pathway.* American Journal of Respiratory Cell and Molecular Biology, 2004. **30**(1): p. 76-83.
31. Wang, Y.L., et al., *Strain-induced fetal type II epithelial cell differentiation is mediated via cAMP-PKA-dependent signaling pathway.* American Journal of Physiology-Lung Cellular and Molecular Physiology, 2006. **291**(4): p. L820-L827.
32. Smith, P.G., K.E. Janiga, and M.C. Bruce, *STRAIN INCREASES AIRWAY SMOOTH-MUSCLE CELL-PROLIFERATION.* American Journal of Respiratory Cell and Molecular Biology, 1994. **10**(1): p. 85-90.
33. Chess, P.R., L. Toia, and J.N. Finkelstein, *Mechanical strain-induced proliferation and signaling in pulmonary epithelial H441 cells.* American Journal of Physiology-Lung Cellular and Molecular Physiology, 2000. **279**(1): p. L43-L51.
34. Chaturvedi, L.S., H.M. Marsh, and M.D. Basson, *Src and focal adhesion kinase mediate mechanical strain-induced proliferation and ERK1/2 phosphorylation in human H441 pulmonary epithelial cells.* Am J Physiol Cell Physiol, 2007. **292**(5): p. C1701-1713.
35. dos Santos, C.C., et al., *DNA microarray analysis of gene expression in alveolar epithelial cells in response to TNF{alpha}, LPS, and cyclic stretch.* Physiol. Genomics, 2004. **19**(3): p. 331-342.
36. Copland, I.B. and M. Post, *Stretch-activated signaling pathways responsible for early response gene expression in fetal lung epithelial cells.* Journal of Cellular Physiology, 2007. **210**(1): p. 133-143.
37. Torday, J.S.P., J.M. Sanchez-Esteban, and L.P.M. Rubin, *Paracrine Mediators of Mechanotransduction in Lung Development.* American Journal of the Medical Sciences, 1998. **316**(3): p. 205-208.
38. Kitterman, J.A., *The effects of mechanical forces on fetal lung growth.* Clinics in Perinatology, 1996. **23**(4): p. 727-&.
39. Chess, P.R., et al., *Reactive oxidant and p42/44 MAP kinase signaling is necessary for mechanical strain-induced proliferation in pulmonary epithelial cells.* Journal of Applied Physiology, 2005. **99**(3): p. 1226-1232.
40. Sanchez-Esteban, J., et al., *Pre- and postnatal lung development, maturation, and plasticity - Cyclic mechanical stretch inhibits cell proliferation and induces apoptosis in fetal rat lung fibroblasts.* American Journal of Physiology-Lung Cellular and Molecular Physiology, 2002. **282**(3): p. L448-L456.
41. Liu, M., et al., *STIMULATION OF FETAL-RAT LUNG-CELL PROLIFERATION INVITRO BY MECHANICAL STRETCH.* American Journal of Physiology, 1992. **263**(3): p. L376-L383.
42. Liu, M.Y., et al., *MECHANICAL STRAIN-ENHANCED FETAL LUNG-CELL PROLIFERATION IS MEDIATED BY PHOSPHOLIPASE-C AND PHOSPHOLIPASE-D AND PROTEIN-KINASE-C.* American Journal of Physiology-Lung Cellular and Molecular Physiology, 1995. **268**(5): p. L729-L738.

43. Liu, M., et al., *The Effect of Mechanical Strain on Fetal Rat Lung Cell Proliferation: Comparison of Two- and Three-Dimensional Culture Systems.* In Vitro Cellular & Developmental Biology. Animal, 1995. **31**(11): p. 858-866.
44. Xu, J., et al., *Mesenchymal determination of mechanical strain-induced fetal lung cell proliferation.* American Journal of Physiology-Lung Cellular and Molecular Physiology, 1998. **275**(3): p. L545-L550.
45. He, Z., et al., *Strain-induced mechanotransduction through primary cilia, extracellular ATP, purinergic calcium signaling, and ERK1/2 transactivates CITED2 and downregulates MMP-1 and MMP-13 gene expression in chondrocytes.* Osteoarthritis Cartilage, 2016. **24**(5): p. 892-901.
46. Chapman, G.B., et al., *Physiological cyclic stretch causes cell cycle arrest in cultured vascular smooth muscle cells.* Am J Physiol Heart Circ Physiol, 2000. **278**(3): p. H748-754.
47. Sedding, D.G., et al., *Mechanosensitive p27(Kip1) regulation and cell cycle entry in vascular smooth muscle cells.* Circulation, 2003. **108**(5): p. 616-622.
48. Liao, X.D., et al., *Mechanical stretch induces mitochondria-dependent apoptosis in neonatal rat cardiomyocytes and G(2)/M accumulation in cardiac fibroblasts.* Cell Research, 2004. **14**(1): p. 16-26.
49. Kroon, A.A., et al., *Prolonged Mechanical Ventilation Induces Cell Cycle Arrest in Newborn Rat Lung.* Plos One, 2011. **6**(2).
50. Bishop, J.E., et al., *CYCLIC MECHANICAL DEFORMATION STIMULATES HUMAN LUNG FIBROBLAST PROLIFERATION AND AUTOCRINE GROWTH-FACTOR ACTIVITY.* American Journal of Respiratory Cell and Molecular Biology, 1993. **9**(2): p. 126-133.
51. Smith, P.G., R. Garcia, and L. Kogerman, *Strain Reorganizes Focal Adhesions and Cytoskeleton in Cultured Airway Smooth Muscle Cells.* Experimental Cell Research, 1997. **232**(1): p. 127-136.
52. Edwards, Y.S., et al., *Cyclic stretch induces both apoptosis and secretion in rat alveolar type II cells.* Febs Letters, 1999. **448**(1): p. 127-130.
53. Park, M.T. and S.J. Lee, *Cell cycle and cancer.* Journal of Biochemistry and Molecular Biology, 2003. **36**(1): p. 60-65.
54. Vermeulen, K., D.R. Van Bockstaele, and Z.N. Berneman, *The cell cycle: a review of regulation, deregulation and therapeutic targets in cancer.* Cell Proliferation, 2003. **36**(3): p. 131-149.
55. Cortez, D., et al., *ATR and ATRIP: Partners in checkpoint signaling.* Science, 2001. **294**(5547): p. 1713-1716.
56. D'Angiolella, V., et al., *The spindle checkpoint requires cyclin-dependent kinase activity.* Genes & Development, 2003. **17**(20): p. 2520-2525.
57. Takahashi, T., et al., *p53: a frequent target for genetic abnormalities in lung cancer.* Science, 1989. **246**(4929): p. 491.
58. Mitsudomi, T., et al., *p53 gene mutations in non-small-cell lung cancer cell lines and their correlation with the presence of ras mutations and clinical features.* Oncogene, 1992. **7**(1): p. 171-80.
59. Dash, B.C. and W.S. El-Deiry, *Phosphorylation of p21 in G2/M promotes cyclin B-Cdc2 kinase activity.* Molecular and Cellular Biology, 2005. **25**(8): p. 3364-3387.
60. Wuerzberger-Davis, S.M., et al., *Enhanced G(2)-M arrest by nuclear factor-kappa B-Dependent p21(waf1/cip1) induction.* Molecular Cancer Research, 2005. **3**(6): p. 345-353.
61. Liu, J., et al., *NF-kappa B responds to mechanical strains in osteoblast-like cells, and lighter strains create an NF-kappa B response more readily.* Cell Biology International, 2007. **31**(10): p. 1220-1224.
62. Chen, Q., et al., *Cyclin B1 is localized to unattached kinetochores and contributes to efficient microtubule attachment and proper chromosome alignment during mitosis.* Cell Research, 2008. **18**(2): p. 268-280.
63. Shoham, N. and A. Gefen, *The influence of mechanical stretching on mitosis, growth, and adipose conversion in adipocyte cultures.* Biomech Model Mechanobiol, 2012. **11**(7): p. 1029-45.
64. Nelson, C.M. and C.S. Chen, *VE-cadherin simultaneously stimulates and inhibits cell proliferation by altering cytoskeletal structure and tension.* J Cell Sci, 2003. **116**(Pt 17): p. 3571-81.
65. Nelson, C.M. and C.S. Chen, *Cell-cell signaling by direct contact increases cell proliferation via a PI3K-dependent signal.* FEBS Lett, 2002. **514**(2-3): p. 238-42.
66. Taieb, F., J.-P. Nougayrède, and E. Oswald, *Cycle Inhibiting Factors (Cifs): Cyclomodulins That Usurp the Ubiquitin-Dependent Degradation Pathway of Host Cells.* Toxins, 2011. **3**(4): p. 356-368.

67. Zhang, X., et al., *N-Cadherin Expression Is Associated with Acquisition of EMT Phenotype and with Enhanced Invasion in Erlotinib-Resistant Lung Cancer Cell Lines.* PLoS ONE, 2013. **8**(3): p. e57692.
68. Uramoto, H., et al., *Epithelial-mesenchymal transition in EGFR-TKI acquired resistant lung adenocarcinoma.* Anticancer Res, 2010. **30**(7): p. 2513-7.
69. Lin, Y., X. Wang, and H. Jin, *EGFR-TKI resistance in NSCLC patients: mechanisms and strategies.* Am J Cancer Res, 2014. **4**(5): p. 411-35.
70. Witta, S.E., et al., *Restoring E-cadherin expression increases sensitivity to epidermal growth factor receptor inhibitors in lung cancer cell lines.* Cancer Res, 2006. **66**(2): p. 944-50.
71. Barr, M.P., et al., *Generation and Characterisation of Cisplatin-Resistant Non-Small Cell Lung Cancer Cell Lines Displaying a Stem-Like Signature.* PLoS ONE, 2013. **8**(1): p. e54193.
72. Collection, A.T.C. *ATCC Cell Lines by Gene Mutation*. 2014 2014; Available from: https://www.atcc.org/~/media/PDFs/Culture Guides/Cell_Lines_by_Gene_Mutation.ashx.
73. Du, L., et al., *Transcriptome profiling reveals novel gene expression signatures and regulating transcription factors of TGFβ-induced epithelial-to-mesenchymal transition.* Cancer Medicine, 2016. **5**(8): p. 11.
74. (NCCN), N.C.C.N., *Clinical Practice Guidelines in Oncology: Colon cancer*. 2016.
75. Langer, C.J., *Roles of EGFR and KRAS Mutations in the Treatment Of Patients With Non–Small-Cell Lung Cancer.* Pharmacy and Therapeutics, 2011. **36**(5): p. 263-279.
76. Ferté, C., et al., *Durable responses to Erlotinib despite KRAS mutations in two patients with metastatic lung adenocarcinoma.* Annals of Oncology, 2010. **21**(6): p. 1385-1387.
77. Huang, Y.-m. and C. Kwiatkowski, *The role of high-throughput mini-bioreactors in process development and process optimization for mammalian cell culture.* Pharmaceutical Bioprocessing, 2015. **3**(6): p. 397-410.
78. Rogers, R.S., et al., *Proteomics Analyses of Human Optic Nerve Head Astrocytes Following Biomechanical Strain.* Molecular & Cellular Proteomics : MCP, 2012. **11**(2): p. M111.012302.
79. Orton, D.J., et al., *Proteomic analysis of rat proximal tubule cells following stretch-induced apoptosis in an in vitro model of kidney obstruction.* Journal of Proteomics, 2014. **100**: p. 125-135.
80. Huang, C., *Hypertension, Mechanical Force, and Renal Disease.* Annals of Clinical and Experimental Hypertension, 2014. **2**(1).